ADDIS ABABA UNIVERSITY

ADDIS ABABA INSTITUTE OF TECHNOLOGY

SCHOOL OF CIVIL AND ENVIRONMENTAL ENGINEERING

The Effect of Corrosion on the Expansion of Concrete

A Thesis in Structural Engineering

By Ezekel Zeleke

January 17,2020

Addis Ababa

A Thesis

Submitted in Partial Fulfillment of the Requirements for the Degree of Master of Science

The undersigned have examined the thesis entitled '**The effect of corrosion on the expansion of concrete**' presented by **Ezekel Zeleke**, a candidate for the degree of **Master of Science** and hereby certify that it is worthy of acceptance.

Dr Esayas Gebreyouhannes		
Advisor	Signature	Date
Dr.- Ing Adil Zekaria		
Internal Examiner	Signature	Date
Dr Asnake Adamu		
External Examiner	Signature	Date
Dr.-Ing Mebruk Mohammed		
Chair person	Signature	Date

UNDERTAKING

I certify that research work titled "**The effect of corrosion on the expansion of concrete**" is my own work. The work has not been presented elsewhere for assessment. Where material has been used from other sources it has been properly acknowledged / referred.

Signature of Student

Ezekel Zeleke

ABSTRACT

Corrosion of reinforcement embedded in concrete is a major concern for the durability of concrete. Its effect is seen through tensile strain development, loss of bond between concrete and rebar or the reduction in the cross-sectional area of the reinforcement. The corrosion products (solid and liquid portion) might exhibit more than six times as compared to the parent rebar. Accordingly, this volumetric expansion of the products causes hoop tensile stress on the concrete.

The research tried to investigate the effects of concrete quality, nature of rebar and the clear cover thickness on the expansion experienced by concrete specimens when reinforcements within them corrode.

A total of fifteen cylindrical concrete samples having a central reinforcement running through them were prepared for three different water to cement ratios. Out of the fifteen samples, six of them had 45mm clear cover while the rest had 28mm. The samples were prepared to alleviate end effect using corrosion resistant epoxy.

To figure out a proper accelerated corrosion test (ACT) set-up, three trial corrosion tests were carried out. Finally, a suitable test set-up was devised and the ACTs of the samples were grouped into four and were performed.

After the analysis of the experimental outputs, it was found that as the water cement ratio increases the strain due to corrosion increased for 28mm clear cover samples and the contrary was the case for the samples with 45mm cover. Also, the clear cover thickness of samples affected the strain development and this effect was seen to be massive for samples with the highest water to cement ratio.

In addition, samples with plane bars showed a slight resilience against corrosion. However, once corrosion started along the surface of plane bars, the strain development is rapid and for the lowest water to cement ratio this was more pronounced.

Key words: Corrosion, Reinforcement, Expansion, Accelerated corrosion test

ACKNOWLEDGMENTS

I would like to express my sincere gratitude to my advisor and mentor Dr Esayas Gebreyouhannes for helping me every step of the way on the fruition of this research. I have to say that your courage and motivation is contagious.

Also, I would like to thank Ato Getachew from School of Electrical Engineering, Ato Anteneh from School of Mechanical Engineering and Ato Faysel from School of Chemical Engineering for their massive contribution in the research.

My stay at the material laboratory was long and draining but Bilelegn, Wubet, Emebet, Demise and Fikru had made it bearable and fruitful. I thank you for that.

Special thanks to Mohammed Siraj, for helping me in the lab when I had difficulties and for helping me in the editorial process of this paper.

Finally, I would like to thank my family, friends and my significant other for their kind words and help through my bitter times.

TABLE OF CONTENTS

LIST OF TABLES

LIST OF FIGURES

ABBREVIATIONS

ACT	Accelerated Corrosion Test
ASTM	American Society for Testing and Materials
A	Ampere
C	Carbon
cm	Centi Meter
DC	Direct Current
ERA	Ethiopian Road Authority
gm	Gram
Fe	Iron
Kg	Kilo gram
Mn	Manganese
MPa	Mega Pascal
μA	Micro Ampere
mA	Milli Ampere
mm	Milli Meter
N	Nitrogen
P	Phosphorous
PVC	Poly Vinyl Chloride
pH	Power of Hydrogen
SSD	Saturated Surface Dry
Si	Silicon
NaCl	Sodium Chloride
NaOH	Sodium hydroxide
S	Sulphur
UTM	Universal Testing Machine

CHAPTER 1 INTRODUCTION

1.1 General Background

Reinforcement corrosion is one of the major factors in the deterioration of reinforced concrete structures, such as bridges, parking, coastal structures and even buildings at times. This phenomenon may lead to an area reduction of rebars, cracking, concrete scaling, reduction of bond strength and change in the bond-slip behavior between concrete and rebars. All of these factors will eventually lead to the adverse function of concrete structures.

The effect of corrosion become highly noticed when de-icing salts started being used in highways and bridges. According to a report (Highway, 1997), about 101,518 bridges of the 581,862 bridges in USA were rated as structurally deficient, and corrosion of the reinforcing steel is a significant contributor to the structural deficiencies. The average annual cost, through year 2011, for just maintaining the overall bridge conditions in US is estimated to be $5.2 billion (Transportation, 2010). And recent studies show that even higher figures are being spent on corrosion maintenance.

The effect of corrosion, though not as severe, is also evident in Ethiopia. Especially on bridges in the low land parts of the country as there is a high deposit of salt in these areas. Data from ERA archive depict that many bridges in the Adigrat and kombolcha district have shown cover scaling (rebar exposure) and corrosion staining on the decks, girders, piers or the combination of these.

Hydrated cement provides such an environment, the normal pH value being 12.6, at which steel is protected in the absence of aggressive anions. At this pH value a passive film forms on the steel that reduces the rate of corrosion to a very low and harmless value. Thus, concrete cover provides chemical as well as physical protection to the steel. However, circumstances do arise in which corrosion of reinforcement occurs due to the ingression of corrosive agents.

Since rust has a larger volume than the steel from which it is formed, the result of corrosion can be cracking, rust-staining, or even spalling of the concrete cover. Such occurrences usually arise from the loss of alkalinity in the immediate vicinity of the steel or from the

presence of excessive quantities of aggressive anions in the concrete (usually chloride), or from a combination of both of these factors.

1.2 Motivation

Providing concrete cover is vital for protecting the reinforcement from environment attack and helps in the bond development between the steel rebar and the concrete. Having these in mind, our building code has forwarded empirical equations that can be used for calculating the concrete cover that should be provided for different types of cases. One of which is for durability. By durability, the concrete cover ensures the rebar is safe against any attack from corrosive agents and minimizes the chance of occurrence of carbonation.

Not few construction building sites observed in Addis Ababa have disregarded the importance of concrete cover. Slabs and beams are cast without any bottom or side spacers and the protection of the reinforcement is solely given to the paste that covers the rebar during vibration. But the paste thickness will not be enough to serve as a concrete cover; hence the risk of corrosion of reinforcement is evident.

Also, many bridges in Ethiopia are facing damages related to corrosion of embedded reinforcement. The maintenance cost to give remedial measures to these bridges and their components is quite large as maintenance measures are taken after significant damage has occurred.

Even though the effects of corrosion of reinforcement takes time to be noticeable, its effect is devastating on the integrity of structures. This research tries to see the mechanism how corrosion of reinforcements compromises the durability of concrete regarding the tensile stress (expansion) it creates on concrete.

1.3 Statement of the Problem

Corrosion of reinforcement has adverse effects on the concrete surrounding it. This emanates from the extensive expansion that occurs during the corrosion of the rebars. Several studies have been done in order to define the corrosion level critical for the cracking of concrete. But these studies' strain measurement techniques have produced scattered and at times bizarre readings. This research will also try to determine the level

of expansion (strain) that results due to the corrosion of the embedded reinforcement. However, the strain measurement, in this case, will be done indirectly using metallic hoops installed on the perimeter of the concrete samples.

1.4 Objective of the research

The objective of this thesis is to estimate, to a reliable degree, the level of expansion that concrete experiences due to reinforcement corrosion through experimental procedure. The expansion of concrete is seen for different concrete strengths, clear concrete covers and surface nature of rebars.

1.5 Scope of the research

This thesis focuses on the expansion experienced by concrete while the reinforcement within corrodes. And the corrosion considered in the research is chlorine induced corrosion only, corrosion due to carbonation of the pore solution is not discussed. Also, time dependent characteristics of concrete are not considered

1.6 Significance of the research

In the fruition of this thesis, it will help to

- Understand the mechanism of stress development that results due to corrosion of embedded reinforcement in the concrete.
- Better understand the corrosion level that leads to crack initiation and propagation in concrete members.
- Layout a proper schedule for corrosion maintenance for concrete structures exposed to corrosive environment.

1.7 Organization of the research

This thesis consists of five chapters and two annexes.

This chapter (chapter 1) being an introductory part includes the objective, scope and significance of the research. The rest of the chapters are discussed in some detail as follow.

Chapter 2 covers the numerous literatures and early works done on and around this thesis's topic. These works help as stepping stones for the chapters to follow.

Chapter 3 addresses the experimental program used in doing the research. The materials, formwork, samples and test set-ups are discussed.

Chapter 4 is devoted to a discussion about the findings of the experiments. It consists of a thorough analysis about the different lines of experiments performed in the laboratory.

Chapter 5 forwards conclusions based on the findings and puts recommendations for future works.

Annex-A provides the properties of the materials used in the research.

Annex-B shows the mix proportions of the different concrete grades used in the research.

CHAPTER 2 LITRATURE REVIEW

2.1 General Introduction

Corrosion of reinforcement is one of the major causes of degradation of concrete structures and loss of durability. This highly increases maintenance cost and shortens the life span of structures. The degradation emanates from the tensile stress the concrete experiences due to the volumetric expansion of the corrosion products. Corrosion usually is initiated by carbonation or with the ingression of high amount of chloride ions into the pore solution. But rarely some other corrosive agents like bromides, cyanates or the variation of the environment (air gaps and voids) along the length of the reinforcement might be the cause for corrosion. [1]

Many offshore structures, bridges, building balconies and roof slabs are usually susceptible to corrosion. This might be due to proper concrete cover being not provided and the ingression of corrosive agents through the cover.

2.2 Mechanism of corrosion of steel in concrete

In general, Corrosion is the spontaneous destruction of metals and alloys caused by chemical, biochemical, and electrochemical interaction between metals and alloys and the environment. Corrosive environments include moisture, oxygen, inorganic and organic acids, high pressure, temperature, and chlorides. During corrosion, metals tend to convert to more thermodynamically stable compounds such as oxides, hydroxides, salts, or carbonates.[2]

Corrosion of steel in reinforced concrete is an electrochemical process that causes the dissolution of iron to form a range of solid products. The products that are made due to corrosion of the steel include complex mixtures of iron oxides, hydroxides, and hydrated oxides according to the prevailing local environment. Also, the volume of these products depends on the level of oxidation and the availability of moisture and it ranges from two to six times the volume of the parent steel. [3]

Fortunately, steel embedded in high pH (more than 9) concrete without the presence of chlorides does not suffer from any severe corrosion attack even if sufficient moisture and

oxygen are available. This is due to the spontaneous formation of a thin protective oxide layer on the steel surface in the highly alkaline pore solution of the concrete. This is called passivation of the reinforcement.

Active corrosion can only commence if this passive layer loses its integrity because of one of the following reasons. The degradation of this protective oxide layer is called depassivation.

- When the pore water in contact with the steel drops to a pH level of about 9 (normally as a result of carbonation).
- And the pore water in contact with the steel contains dissolved chloride ions above a certain threshold level. [4]

2.3 Types of corrosion

There are several types of corrosion according to the general characteristics of the mechanism of corrosion. [5] and [6]

- Uniform (General): It happens consistently all over the surface of the bar. The corrosion rate is commonly given as a weight loss. Uniform corrosion is very common, and is the basis of most predictive mathematical equations for corrosion.
- Galvanic: Corrosion caused by an electrochemical reaction in an electrolyte between two dissimilar metals when placed in contact or electrically attached to each other.
- Crevice: A localized type of corrosion that occurs within the stagnant zones produced between two surfaces by the interfaces.
- Pitting: Pitting corrosion is a localized type of corrosion that continues with limited overall loss of metal making detection difficult. Therefore, it is difficult to predict, and its attack rate is difficult to quantify, since its reaction rate cannot be quantified.
- Selective leaching: An element is preferentially removed from an alloy, leaving a (often porous) residue of the elements more resistant to the particular environment.

- Environmentally Induced Cracking (EIC): is a general term for mechanically brittle failures resulting from a synergy between tensile stress and a corrosive environment. EIC includes stress-corrosion cracking (SCC), corrosion fatigue-cracking (CFC) and hydrogen induced corrosion (HIC)

2.4 Factors affecting corrosion rate

There are numerous factors that affect the corrosion rate. This has made dealing with corrosion very complex. The following are known to affect corrosion rate.

- **Oxygen supply**: As a reactant in the corrosion reaction, the rate of corrosion is directly dependent on the Oxygen's supply to the steel's cathodic region as shown in Figure 2-1. The amount of its supply depends on concrete porosity (P), the degree of moisture content in these pores (RH), the thickness of concrete cover (d) and temperature. [4]

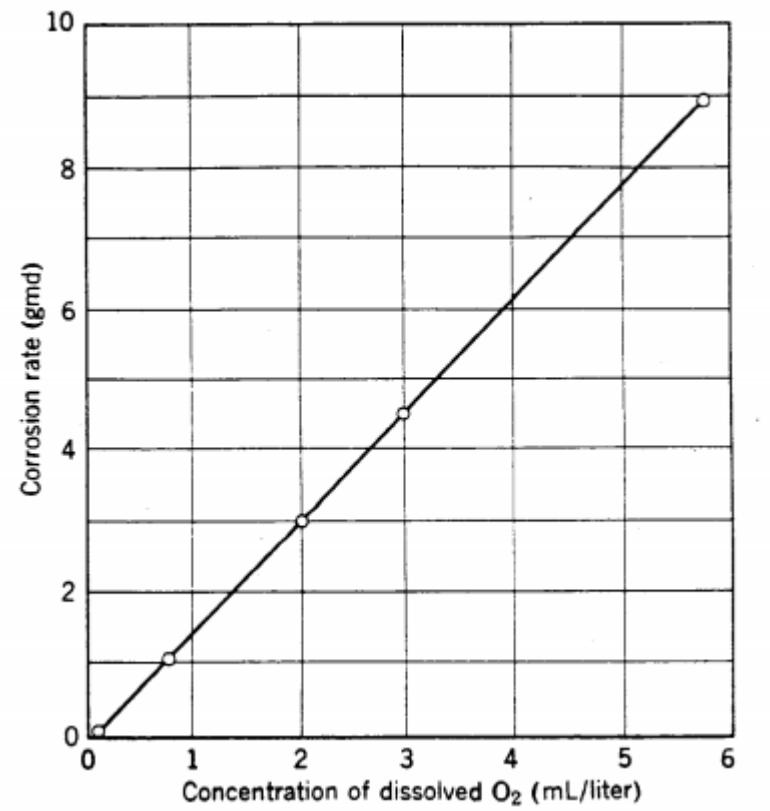

Figure 2-1: Effect of Oxygen supply on corrosion rate [6]

Nevertheless, a lot of research has shown that the moisture content has the greatest impact on the supply of oxygen.[4] The porous system is partially open for atmospherically

exposed concrete structures which allow oxygen to be transported in the gaseous state. Compared with the diffusive oxygen transport in water-filled pores, this transport is fast. The supply of oxygen is so low in fully submerged systems that the corrosion risk becomes very low, even in the presence of high Chlorine concentration. A relative humidity value as high as 95 percent does not greatly restrict the supply of oxygen, but it becomes evident at relative humidity near 100 per cent. It should be noted, however, that extreme pitting can even result in a limited supply of oxygen if the anode / cathode area ratio is high and the resistivity low.

- **Temperature**: A general rule of thumb is that temperature change of 10^{o}C approximately double the rate of chemical reaction. However, the temperature dependency may be altered by other non-chemical parameters involved in the overall reaction (e.g., resistivity). Nevertheless, the corrosion rate increases dramatically with increment in temperature in normal ambient temperature range, but at high temperature (probably about 40^{o}C), the corrosion rate begins to decrease due to lack of oxygen (solubility of oxygen decreases with higher temperature). [4]

- **Relative humidity**: It affects the rate of corrosion in three different ways.

    - Only in liquid water can the corrosion reaction occur, as water is a reactant absorbed in the reaction. This requires minimum moisture in the pores that is in contact with the steel. The electrochemical reaction ceases when pores dry out.

    - The rate of corrosion depends on the supply of oxygen which in turn depends on the concrete's moisture content.

    - The rate of Corrosion depends on the concrete's electrical resistivity. Also, resistivity depends on the concrete's moisture content.

- **Chloride concentration**: Depassivation occurs when chloride ion concentration dissolved in pore water reach a threshold value. The active corrosion rate increases by increasing the amount of chloride present as shown in Figure 2-2, i.e. the number of pits can increase, resulting in nearly uniform corrosion.

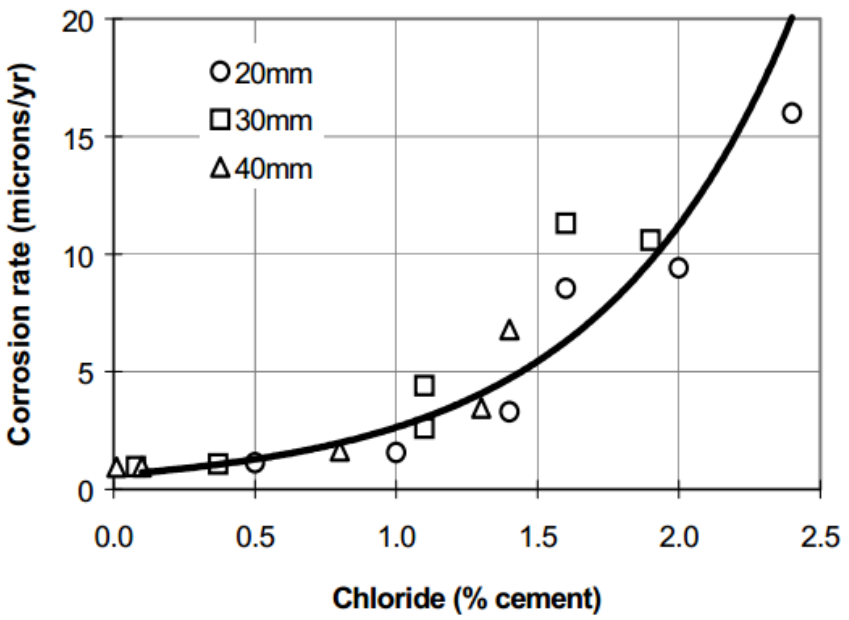

Figure 2-2: Effect chlorine concentration on the corrosion rate for different cover thickness [6]

Steel corrosion in a NaCl solution initially increases up to around 3 percent due to enhanced conductivity of the solution (depicted in Figure 2-3). Much higher concentration of dissolved salt however decreases the solubility of oxygen and the risk of corrosion decreases steadily.

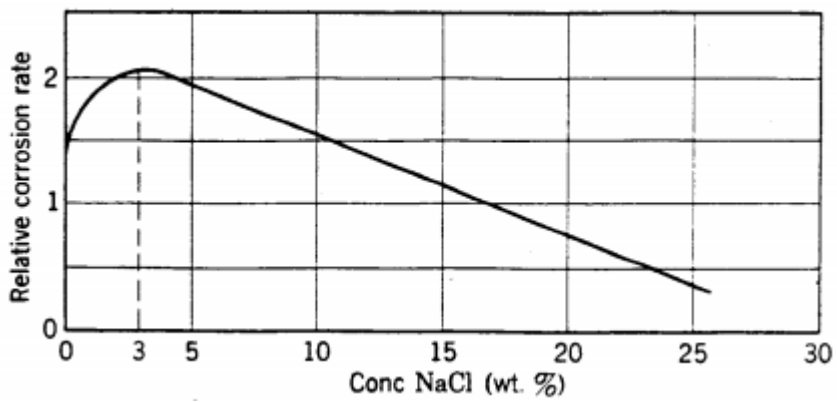

Figure 2-3: Effect of concentration of NaCl in the pore solution on corrosion rate

- **PH**: It affects the corrosion rate in four different ways. It affects the passivity of steel; a decrease in PH increases the solubility of chloride which will in turn

increase corrosion rate; a decrease in PH increases the cell potential between anode and cathode; on top these lowering of PH increases $[Cl^-]/[OH^-]$ ratio which will result increased corrosion rate.

- **Resistivity**: Low-resistivity supports ion migration. Low resistivity also favors the development of corrosion pits, and the ratio of cathode / anode area can grow very large. The amount of moisture in the pores influences the resistivity considerably. The higher the moisture content and ionic strength, the lower the resistivity.

2.5 Nature of corrosion products

In studies carried out on the atmospheric corrosion of steel there are nine phases of iron oxide that are present in the corrosion coating on steel. These phases are iron hydroxide (Fe(OH)), iron trihydroxide ($Fe(OH)_3$), goethite (α-FeOOH), akaganeite (β-FeOOH), lepidocrocite(γ-FeOOH), feroxyhite (δ-FeOOH), hematite (α-Fe_2O_3), maghemite (γ-Fe_2O_3) and magnetite (Fe_3O_4). Figure 2-4 illustrates the volumetric expansion of corrosion products compared to bare iron.

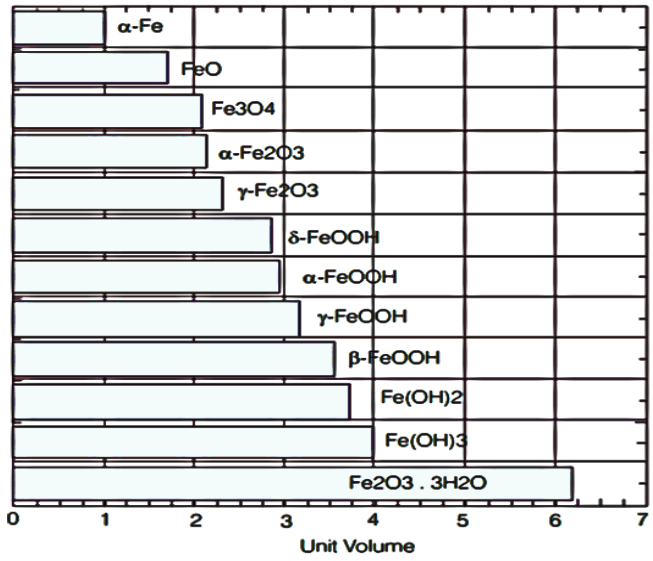

Figure 2-4: Comparison of volumes of corrosion products and parent metal [7]

The nature of the corrosion products depends on several factors including concentration of chlorine, availability of oxygen, pH. The products might be solid precipitates or soluble liquids. [8]

2.6 Natural versus Accelerated corrosion

The corrosion that occurs in structures usually take about ten or more years to cause any visible effects even though it might have commenced awhile back. But it will not be feasible to take this much time in order to study the mechanism and effects of corrosion. As a result, it was found necessary to accelerate this process artificially to get results with a reasonable time limit.

The accelerated corrosion has shown to be 20 times faster than natural corrosion for the investigated geometry and environmental conditions. [9] With respect to Faraday's law, the use of different current densities for ACT has no effect on the percentage of mass loss. However, increasing the level of current density above 200 mA/ cm^2 results in a significant increase in the strain response and crack width due to corrosion of the steel reinforcement.[10] A possible explanation is that the crystallization or precipitation of ionized gel to solids takes some time. [11]

Since the detrimental factor is the portion of the rust that solidifies, an empirical relation (equation 1) was forwarded by Gebreyouhannes et al to estimate the crystalline portion in relation to the current density imposed conservatively. [11]

$$\beta = 0.75 - 0.1 * \log_{10} icorr \leq 0.75 \quad \text{.....(1)}$$

Where: β - is the ratio of crystalized rust around the bar and it is always greater than zero.

i_{corr} - is the corrosion current density in μA/cm^2

Nevertheless, studies show that the total current applied will not be used to induce corrosion. Accordingly, there are equations put forward to calculate the effective current density. One of them is equation 2 given by Austin et al. [12]

$$icorr = \left(\frac{tc*ac}{t*Ac}\right) * iapp \quad \text{.....(2)}$$

where *t* = total time of external current applied; *tc* = duration of the corrosion application; *Ac* = area of rebar over which the current is applied; *ac* = area of the depassivated portion of the rebar; and *iapp* = applied current density (Amp/cm^2)

And Equation 3 is obtained from plotting the data from Azher and Al-Ghoi experiment. [12]

$icorr = 1.95\ln(iapp) + 0.39$, where $iapp \geq 0.82\text{mA/cm}^2$…….(3)

2.7 Previous works

2.7.1 Andrade et al 1993

This work included the accelerated corrosion experiment on four samples prepared with a concrete having water to cement ratio of 0.5. The current densities used in the experiment were 10 and 100 μA/cm^2 that where the maximum densities measured in naturally occurring corrosion. In the experiment, current was assumed to be completely effective. This means that 100% of the current imposed was utilized to induce corrosion on the surface of the bars. Two samples had 2cm clear cover while one sample had 3cm clear cover. And the final sample had its bar positioned at the corner of the concrete having a 2cm and a 3cm clear cover on the adjacent surfaces. However, positioning of the rebar at the corner gave erratic strain gauges as it is possible for cracks to occur on both surfaces with almost equal probability.

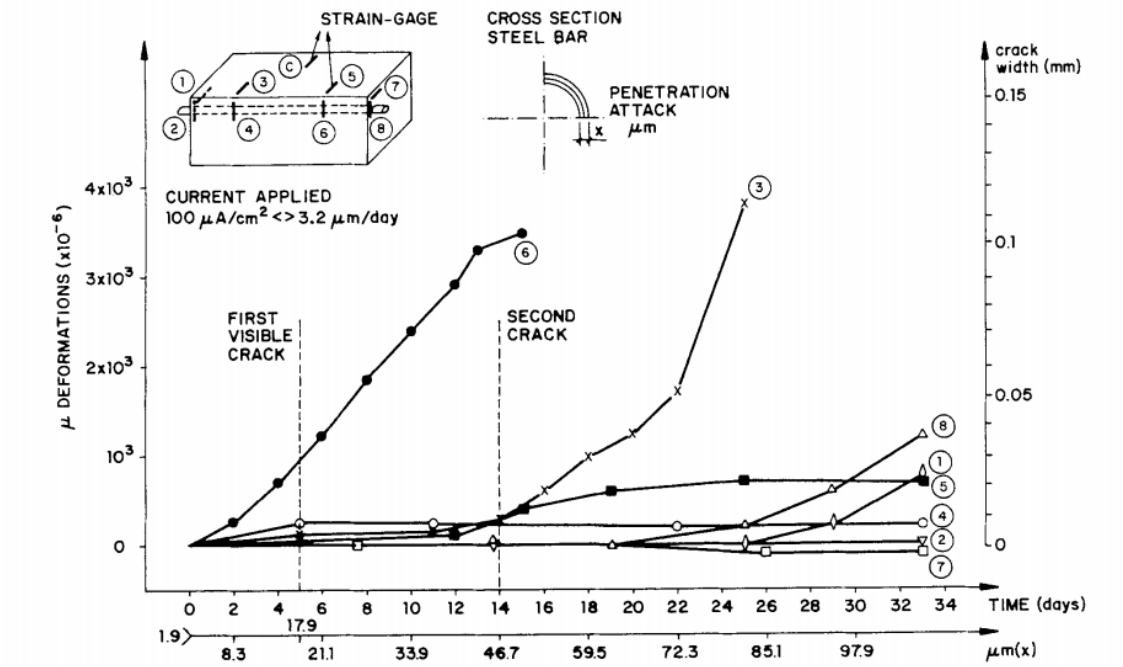

Figure 2-5: Strain readings for the sample with a rebar at the corner

This can be clearly seen on the reading from strain gauge 3 and 6 on figure 2-5. Strain gauge 6 showed higher strain in the early days even if it located on the surface with higher clear cover making it quite peculiar. Afterward, strain gauge 3 depicted development of strain a bit higher than strain gauge 6.

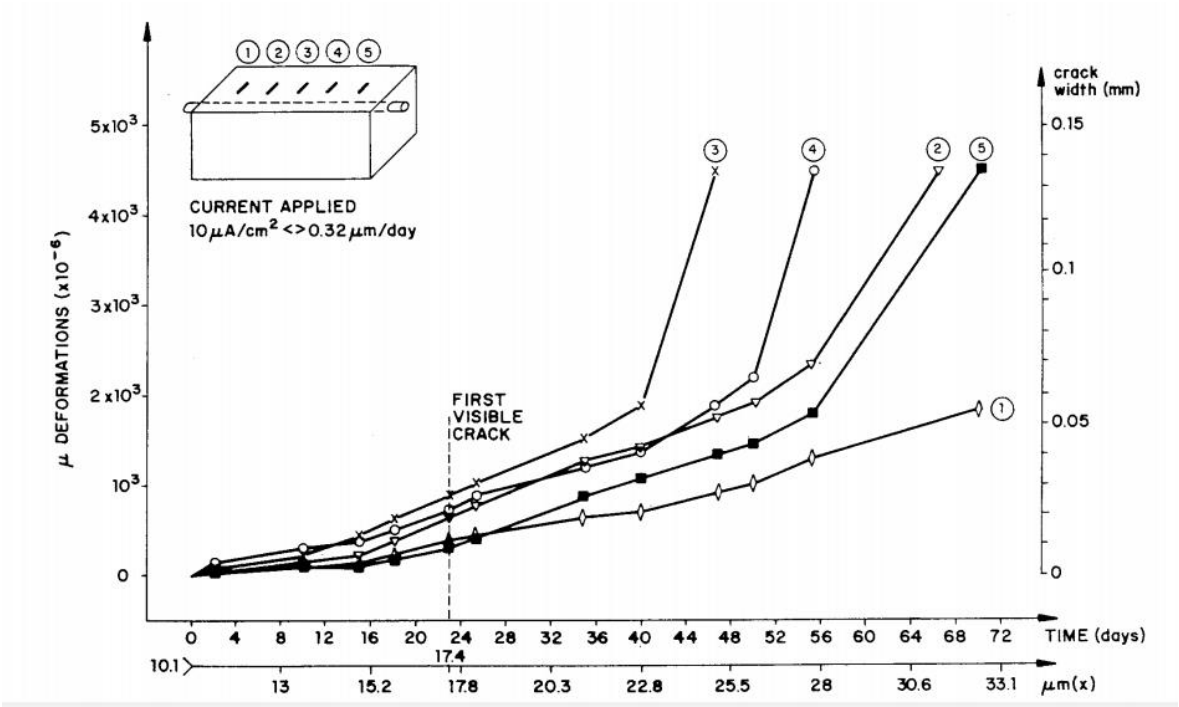

Figure 2-6: Strain readings of the sample with 2cm cover exposed to 10 μA/cm^2 current density

From figure 2.6, it is evident that the strain readings showed much spreading when the current density is lowered.

2.7.2 El Maaddawy & Soudki, 2003

The experimental program used in this paper included twelve samples 300 mm long with a 150X250 mm cross section. Each sample had two 11.3mm diameter bars on two adjacent corners with 25mm clear cover to each face. Two strain gauges were installed above and below the rebars on both sides shown in figure 2-7. The variables in the experiment were the impressed current and the duration of corrosion.

Since the rebars had equal clear cover on both sides, the probability of crack occurring on both sides was the same. Nevertheless, strain gauges were installed on one face only; hence missing to record strain development on the second face.

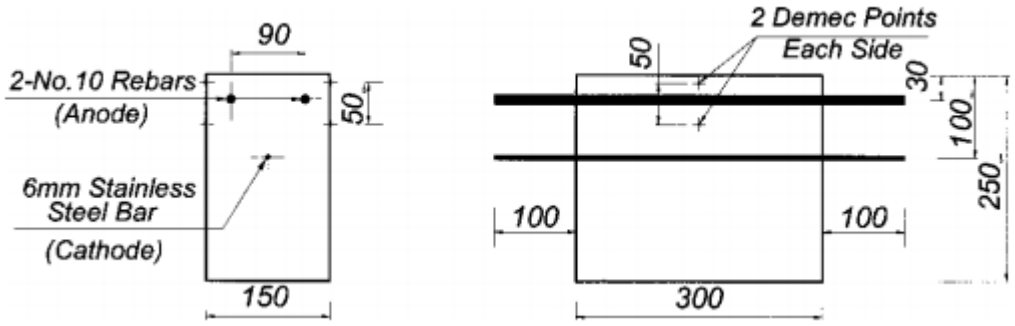

Figure 2-7: El Maaddawy & Soudkis' experiment specimen

And also, from the crack patterns shown in figure 2-8, strain had developed on the upper surface manifesting itself as longitudinal cracks specifically on Type two and Type three crack patterns witnessed during the experiment.

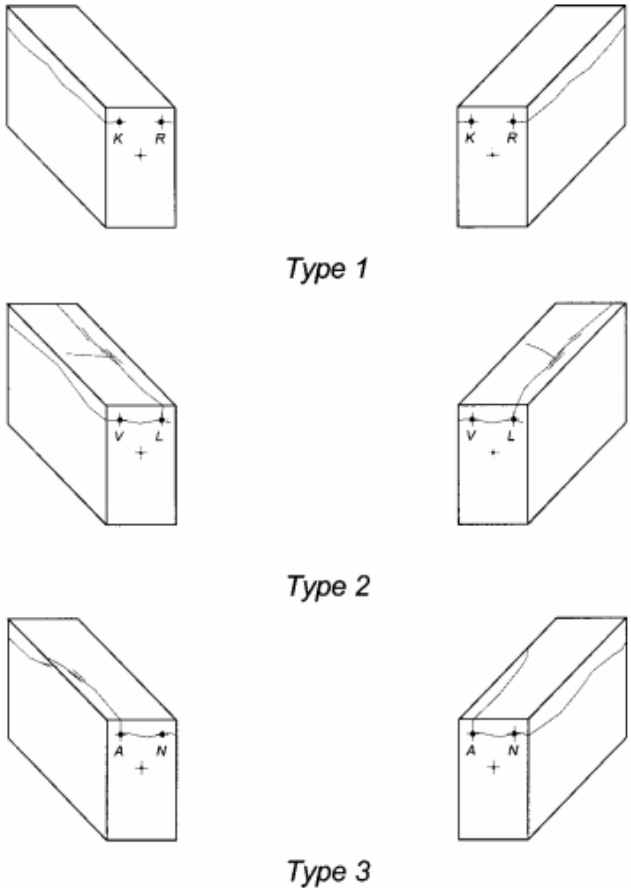

Figure 2-8: Crack patterns due to corrosion

2.7.3 Oh et al, 2009

In the experiment of the research, 200 X 200 X 200mm concrete cubes with a 20mm steel bar running through the samples were prepared as shown in Figure 2-9. The clear cover of the rebar and water to cement ratio were the variables in the experiment. To see the effect of corrosion in great detail, the corrosion region was only limited to the center of the cubes (80mm only). This was done by using PVC pipes and then sealing the gaps with a corrosion-resistant epoxy.

To measure the strain development, a concrete strain gauge was installed on the face near to the rebar. However, the reading was taken every 30 minutes after the ACT commenced.

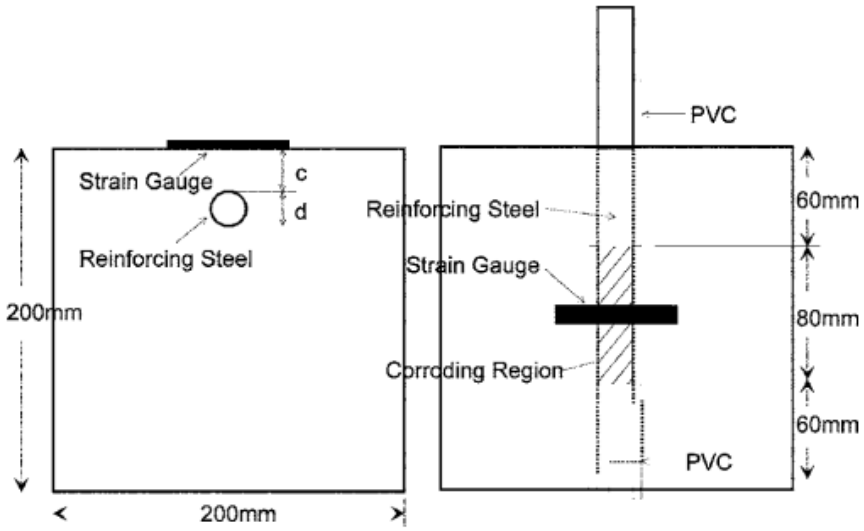

Figure 2-9: Oh et al experiment sample.

The interval of strain reading makes it very difficult to locate the time of cracking as it occurs instantly. As a remedy, crack was assumed to occur when the strain reached the cracking strain obtained from the tensile strength test on the concrete.

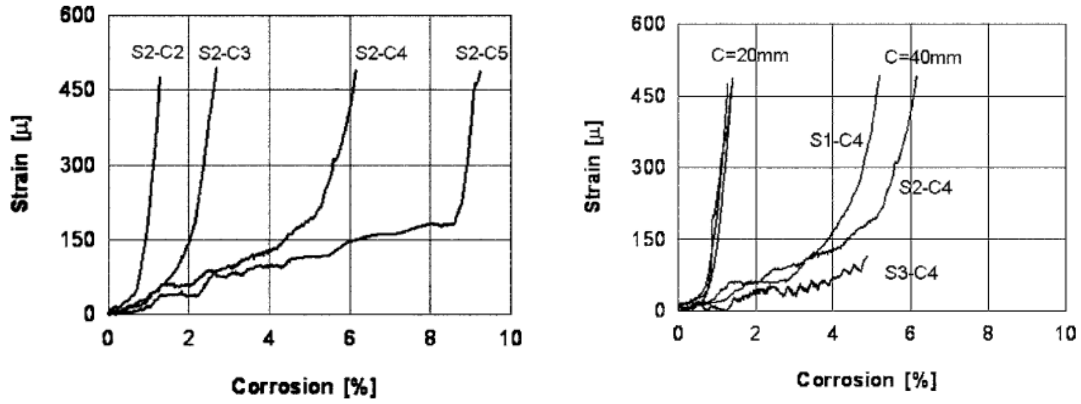

Figure 2-10: Strain versus corrosion percentage

Some portion of the curves in Figure 2-10 show a smooth increment; this might be due to the gap between readings. The time gap failed to capture the sudden strain release as cracking occurred.

2.7.4 Wang et al, 2014

As a mechanism to test the proposed model in the paper, an experiment comprising an ACT on 100 X 100 X 100mm concrete sample of water to cement ratio of 0.5 was prepared. In order to measure the strain induced as corrosion of the rebar undergoes, a group of three strain gauges was posted at a fixed radius as depicted in Figure 2-11, and there were two groups. The strain readings were captured every 10 minutes. The procedure followed to find the time of cracking of the samples is not stated.

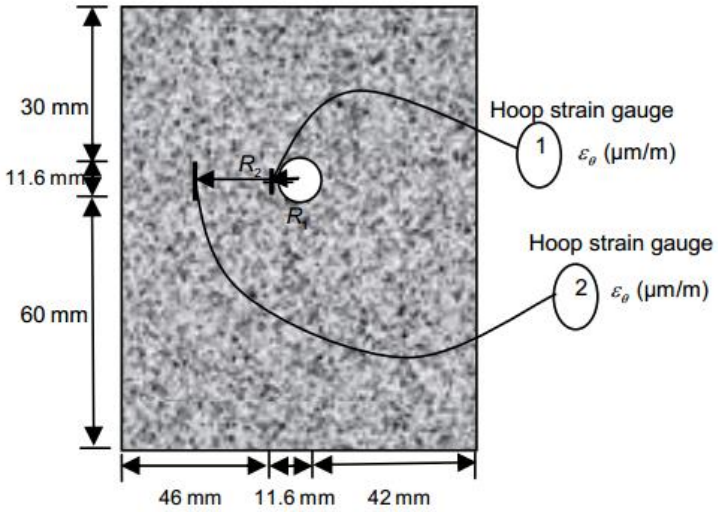

Figure 2-11: Wang et al experiment sample

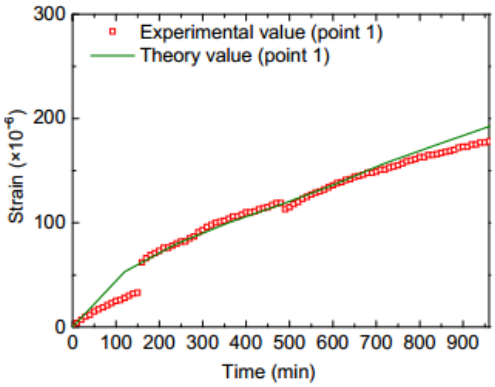

Figure 2-12: Strain at point 1

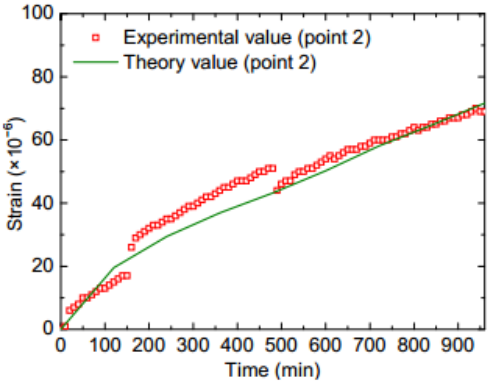

Figure 2-13: Strain at point 2

From Figure 2-12 and 2-13 it can be seen that the theoretical and experimental values conform well for most part of the duration especially after 500 minutes.

The cover thickness on four sides of the corroding rebar; hence, the hoop-strain is different on each side of the rebar. As a result, installing point strain gauges in the concrete sample might give erroneous reading.

2.7.5 Altoubat et al, 2016

The experiment program of the research included two portions. The first was to carry out both constant voltage and constant current ACT on steel reinforced columns to about a degree of corrosion of 8%. Then the columns were loaded to failure with a centric loading.

Ends of the sample were coated with corrosion-resisting epoxy to concentrate the corrosion in the middle and minimize end effect shown in Figure 2-14. Two strain gauges were mounted horizontally at the center of the sample 180˚ apart to measure and see the strain variation to measure the circumferential strain during loading. In addition, one longitudinal strain gauge was installed at the center for measuring axial deformation in addition to transducers.

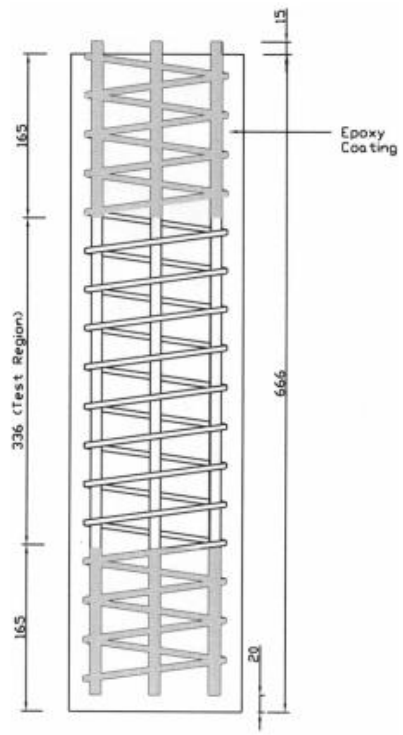

Figure 2-14: Rib cage of the columns

However, a specially designed and fabricated mechanical expansion collar, shown in Figure 2-15, was used to measure the circumferential strain during the ACT.

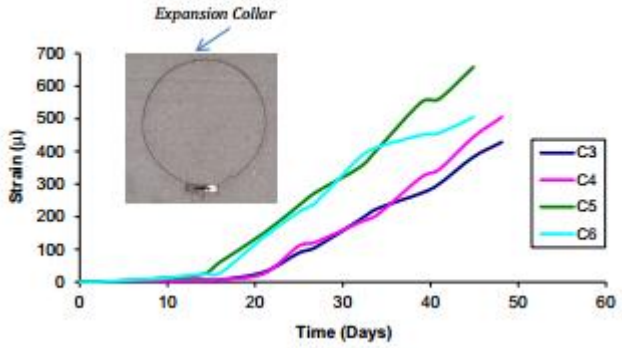

Figure 2-15: Expansion collar and their strain readings

These collars were installed at the top and bottom of the corroding region. However, the expansion at the center of the samples had not been measured. However, since the expansion collar circumscribes the circular columns, the maximum strains the concrete experienced when the rebar with in corroded at the installed locations were captured.

2.8 Research gap

The corrosion of reinforcement embedded in concrete structures has been a topic of several researches as the mechanism how it affects the integrity of concrete is not known to a satisfactory level. And also, most empirical and semi-empirical approaches forwarded to quantify its effects fail to give consistent results for different lines of experiment results.

Hoop strain resulted from corrosion of rebar due to the corrosion products will follow the path that possess the weakest tensile strength (along the shortest cover) then a crack will emerge. Therefore, installing point strain gauges to capture the strain development will lead to erratic readings.

Cracking occurs when the tensile capacity of the concrete is exceeded by the hoop stress-induced as a result of the relative expansion of the corrosion products. This process is sudden and it is followed by a quick reduction of strain due to the release of the corrosion products through the crack. Since it will take so much strain data acquisition refinement, the time to crack is obtained in most researches from the cracking strain obtained from cylindrical or flexural tests conducted on the side. When the strain reading on the concrete exceeds the cracking strain from the side tests, it will be taken as the time of cracking.

However, during ACT the concrete will be submerged in a saline solution. Even if, it differs with the current density, this submersion might affect the compressive and tensile strength of the concrete. [18] In addition, the straining rate will also affect the mechanical properties of concrete. [19]

CHAPTER 3 EXPERIMENTAL PROGRAM

In this chapter, the experimental program followed to see the effects of concrete quality, clear cover thickness and surface nature of rebars on the hoop tensile strain developed due corrosion is discussed. The program is mainly an accelerated corrosion test on a cylindrical concrete sample that has a central reinforcing bar running through it. The aim of the experiment was to measure the amount of expansion (strain) experienced by concrete to a more accurate level when corrosion of reinforcement is taking place. The main variables being studied are water to cement ratio and concrete clear cover. But also, three samples with plane bars of equivalent diameter were prepared for the three water to cement ratios to see the effect of the shape of the rebar. A total of fifteen samples were prepared and tested. The samples were grouped into four parts and the experiment was carried out. Detail discussion about the materials used, samples and test set up is done in the following sections.

3.1 Test specimen

The test specimens are 40 cm high cylindrical concrete sections with a Φ16 deformed or equivalent plane rebar placed at the center. The main variable in the samples is water to cement ratio. Accordingly, the samples are classified as shown in Table 3-1.

Table 3-1: Type of test samples

Group	Designation	w/c ratio	Clear cover (mm)	Number of samples	Nature of rebar
A-series	A	0.65	28	2	Deformed
		0.65	45	2	Deformed
	AP	0.65	28	1	Plane
B-series	B	0.5	28	2	Deformed
		0.5	45	2	Deformed
	BP	0.5	28	1	Plane
C-series	C	0.4	28	2	Deformed
		0.4	45	2	Deformed
	CP	0.4	28	1	Plane

The three water to cement ratios were selected to see its effect on the expansion for concrete strengths that are usually encountered on site. On top of this, the gap between the three was thought to help see the effect of water to cement ratio distinctively.

The two clear covers were selected because the two chosen thicknesses resemble the cover thickness mostly provided on site and also for ES-EN 1992:2015's recommendation for minimum thickness of cover for durability of reinforcement steel, the two clear cover thicknesses can be representative for the structures with XC2/XC3 exposure class or worse.

3.2 Materials

3.2.1 Concrete

The concrete for all samples was prepared from the same locally available aggregate and sand after thoroughly studying their properties. While casting the different groups of samples, the only thing allowed to change was water to cement ration while keeping the other variables unchanged as much as practically possible. Binary method of mix design is followed to prepare the concrete samples as given in Table 3-2.

Table 3-2: Mix compositions

Series	W/C ratio	Water (Kg)	Cement (Kg)	Fine aggregate (Kg)	Coarse aggregate (Kg)	Sand/Aggregate ratio*
A	0.65	190	292.31	804.34	1016.28	0.45
B	0.5	190	380.00	772.22	975.70	0.45
C	0.4	200	500.00	716.73	905.59	0.45

** The ratio of volume of sand (fine aggregate) to the total volume of aggregate.*

3.2.1.1 Cement

The cement used for the concrete samples is an Ordinary Portland Cement (OPC Grade-42.5R) from a local provider.

3.2.1.2 Fine aggregate

The fine aggregate used for the research was washed and dried before being stored in plastic sacks to keep moisture change to a minimum. The properties of the fine aggregate are given in the Table 3-3.

Table 3-3: Fine aggregate properties

Property	Laboratory result
Specific gravity (SSD)	2.564
Fineness modulus	2.86
Moisture content	1.57%
Absorption capacity	3.09%

3.2.1.3 Coarse aggregate

Similar to the fine aggregate, the coarse aggregate was washed, dried and then stored with minimum loss and gain of moisture. Table 3-4 summarizes the properties of the coarse aggregate used for all test samples.

Table 3-4: Coarse aggregate properties

Property	Laboratory result
Maximum aggregate size	25mm
Gradation	Well-graded
Size number	6
Specific gravity (SSD)	2.65
Moisture content	1.27%
Absorption capacity	1.52%

Maximum aggregate size of 25mm was selected to avoid aggregate clogging while casting the thinner cylinders. And the coarse aggregate was prepared in the laboratory by sieving and mixing the constituent aggregate sizes according to ASTM C33-03 as given in Table 3-5.

Table 3-5: Gradation of the coarse aggregate

ASTM Passing Range	Sieve size	% passing	% cumulative	% retained
100	25	100	0	0
90-100	19	95	5	5
20-55	12.5	37.5	62.5	57.5
0-15	9.5	7.5	92.5	30
0-5	4.75	0	100	7.5

3.2.1.4 Concrete strengths

Using these input materials and the mix proportion stated, the three series of concrete were prepared. Three compressive cube samples (150X150X150) and nine flexural samples (500X100X100) were taken for each series of concrete. However, as a result of faulty testing three flexural samples from each series were discarded leaving six samples. Accordingly, the six samples were divided into three to see the tensile strength development of the samples at the 28^{th}, 56^{th} and 90^{th} day. The results of the compressive and tensile strengths of samples from each series are summarized in Table 3-6 and 3-7.

In addition, for A-series only cylindrical samples of 150mm diameter and 300mm height were prepared for splitting test. This was done to see the variation between two-point flexural test and splitting test in calculating the tensile strength of the concrete samples. This being said, all analyses and discussions, if any, are based on the two-point bending test results even if it is evident that they give higher tensile results than their splitting counterparts. This is attributed to the fact that a linear stress distribution is assumed by the modulus rupture measurement. [21]

Table 3-6: 28th day compressive strength of the concrete series

Series	Cube	Mass (Kg)	28th-day Compressive Strength (MPa)	Average (MPa)	COV
A	1	7.94	26.58	25.8	0.400422
	2	7.865	25.8		
	3	7.785	25.03		
B	1	7.94	36.38	36.64	0.040289
	2	8.005	36.87		
	3	7.96	36.66		
C	1	7.705	44.49	45.67	1.620556
	2	7.97	47.44		
	3	7.505	45.09		

COV- Coefficient of variation.

Table 3-7: Different age tensile strength of the concrete series

Series	Test method	Tensile strength (MPa)					
		28th day	Average	56th day	Average	90th day	Average
A	Splitting	2.075	2.08	2.63	2.62	2.851	2.73
		2.014		2.6		2.607	
		2.161		-		-	
	COV	0.003636222		0.000225		0.014884	
	Flexural (Two point)	2.774	2.79	3.06	3.24	3.51	3.3
		2.815		3.42		3.094	
		-		-		-	
	COV	0.00042025		0.0324		0.043264	
B	Flexural (Two point)	3.019	3.2	3.234	3.6	3.89	3.97
		3.375		3.965		4.054	
		-		-		-	
	COV	0.031684		0.13359025		0.006724	
C	Flexural (Two point)	3.375	3.375	3.678	4.11	4.95	5.09
		3.375		4.545		5.22	
		-		-		-	
	COV	0		0.18792225		0.018225	

The Two-point flexural tests to calculate the modulus of rupture were done and adjusted according to ASTM C78-02 .

3.2.2 Reinforcement

The reinforcement bars used to prepare the specimens are deformed Φ16 rebars and equivalent plane bars. The yield and the ultimate strength of the rebars are 570MPa and 680MPa respectively.

To compute the equivalent diameter for the Φ16 rebars, the following procedures were carried out. Initially, a deformed Φ16 rebar sample's ribs were removed mechanically and a plane bar of constant diameter (14mm) was obtained. Next both the plane bar and deformed Φ16 rebar were tested until failure in the UTM as shown in Figure 3-1, 3-2 and 3-3 respectively. The yield and ultimate loads were noted for both samples. As the exact area of the plane bar is known, the yield and ultimate stresses can easily be computed. And since these stresses are material properties and both samples are taken from the same reinforcement the equivalent diameter of the deformed Φ16 rebar was obtained using the stresses computed.

Figure 3-1: Test of the Plane bar

Figure 3-2 Test of the Deformed rebar

Table 3-8: Chemical composition of the rebars

Diameter	C (%)	Si (%)	Mn (%)	P (%)	S (%)	N (%)	Fe (%)
Φ20	0.19	0.21	0.61	0.01	0.007	0.004	98.1
Φ16	0.2	0.16	0.71	0.01	0.006	0.004	98

Accordingly, the diameter of the equivalent plane bar to the deformed Φ16 rebar was found to be 16.26mm. Unfortunately, this diameter of the plane bar cannot be prepared from a deformed Φ16 rebar, hence a deformed Φ20 rebar from the same supplier was used. Though the supplier is the same, a chemical composition test was carried out for the deformed Φ16 and the Φ20 samples because the chemical content of reinforcing steel affects its properties under corrosive environment.

Accordingly, the chemical composition of both rebar samples was done and the result given in Table 3-8 shows that the two types of reinforcements have similar chemical composition.

Figure 3-3: Rebar Samples after rupture

3.3 Specimen preparation

As stated above, the specimens used in the ACT are cylindrical concrete samples with a central bar running through and protruding at the top to install the electrical wire required for the experiment as shown in Figure 3-4. The bars in the samples are coated at the top and at the bottom using corrosion-resistant epoxy to avoid end effect. End effect is a phenomenon where the corrosion is highly concentrated at the ends of samples. This may be due to the formation of a short circuit as a result of the water vapor on the rebar and

concrete interface at the ends. Hence, the current will take the short route to the cathode; accordingly, the corrosion will be severe at the ends.

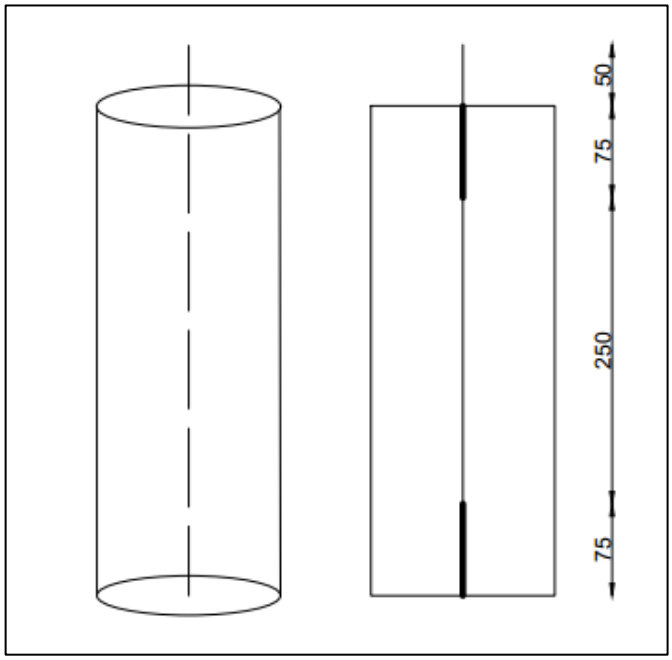

The height of concrete=400mm

Corrosion insulated portion=75mm

The length of rebar protruding at the top=50mm

Diameters of the cylinder are 72mm and 106mm.*

Figure 3-4: Schematic representation of the experiment sample

** These diameters were selected according to the available formwork diameters also.*

The regions identified to be susceptible to end effects were coated with non-corrosive epoxy and checked that the epoxy was by no means damaged before casting as shown in Figure 3-5 and 3-6. Also, the visible portion of the non-corroding region was checked after casting and it was made sure that the rebar has not been revealed.

Figure 3-5: Deformed bars after application of non-corrosive epoxy

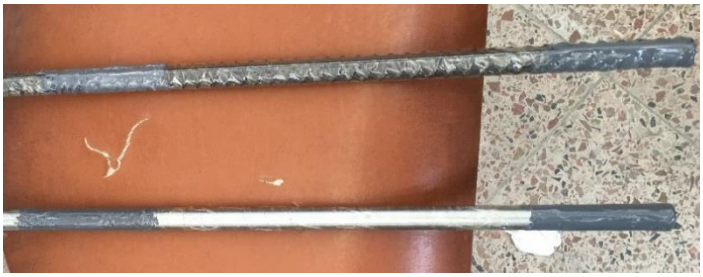

Figure 3-6: Deformed and plane bars after application of non-corrosive epoxy

The formwork used to cast the samples was prepared using a PVC pipe and a base made of iron plate to keep the PVC pipe in place while the concrete is being cast and vibrated as shown in Figure 3-7. In order to keep the reinforcement at the center of the sample, a central hole was prepared on the base plate (Figure 3-9) and at the top tripod-like metal keeps the bar firmly at the center (Figure 3-8).

Figure 3-7: Formworks used in preparing the samples

The PVC pipes used in the formworks were slit longitudinally at one location to ease the removal of concrete after hardening. The opening was then stitched properly using a highly adhesive tape. As a result, the concern of the concrete sample bulging and loss of concrete paste during vibration was addressed satisfactorily.

Figure 3-8: Tripod like metal used to keep the rebar at the center

Figure 3-9: The bases of the formworks and their central hole

During casting, three compressive cubes and nine flexural samples were taken alongside the ACT samples for each water to cement ratio. After twenty-four hours of setting, the concrete samples were removed from their respective formworks and allowed to cure in a tap water-filled tank until the testing day. The dissolved chlorine in tap water is not that much also the rebars protruding at the top are covered with epoxy and tape; hence the risk of corrosion starting in the curing tank before the actual experiment is quite slim. Besides, the scarcity of dissolved oxygen in the curing water will retard any kind of corrosion from happening.

3.4 Test setup and Instrumentation

3.4.1 Accelerated Corrosion Test

Before going about the main ACT experiment, trial tests were deemed necessary because it is vital to keep the corrosion only in the corrosion region and also to compute the degree of corrosion taking place. Since the trials were done to check the appropriateness of the ACT set-up, the samples do not resemble the actual samples of the research.

For trial one, a cylindrical concrete sample having a central reinforcement running through it was prepared and ACT was carried out. In the test setup, the sample was soaked in 3% by mass Sodium Chloride (NaCl) solution and was supplied with constant voltage. A thin aluminum plate was used as a cathode while the reinforcement in the concrete served as an anode as depicted in Figure 3-11. After two days of the inception of the experiment, the sample started exhibiting corrosion products at the two ends of the sample. No surface cracks were visible in the first week, so the voltage was increased regularly and finally set to 30V. A few days later, the sample showed a longitudinal crack along which liquid corrosion products emerged.

Figure 3-10: Split sample after experiment

Figure 3-11: Trial one set-up

In the first trial, the corrosion of the rebar was almost uniform (almost no local or pitting corrosion) along its length except at the ends as shown in Figure 3-10. But the degree of corrosion cannot be estimated using Faraday's law during the experiment as the current is not constant. Also, the aluminum installed as a cathode was worn out halfway through the experiment due to the redox reaction taking place. It had to be replaced two times during the whole experiment. At the end, it was understood that the experiment set-up needed to be modified.

Accordingly, a second trial sample was cast and tested as shown in Figure 3-12. But this time instead of keeping the voltage constant, it was tried to keep the current constant. Unfortunately, the DC power supply available in the laboratory is not capable of doing so rather it can keep the potential constant. But this solely will not guarantee the constant current supply because once corrosion initiates, the overall resistance of the system varies hence causing current fluctuations.

The cathode used in this experiment was a graphite rod. This has alleviated the problem of wearing out of cathode during the experiment as a graphite rod is more resilient.

Figure 3-12: Trial two set-up

The sample showed severe corrosion at the ends but as the current was not kept constant, the set-up was not satisfactory.

Finally, a third sample was prepared for ACT. In the preparation of the sample, non-corrosive epoxy was used to cover the ends of the rebar to prevent end effect as shown in Figure 3-13. And also, a separate circuit, shown in Figure 3-14, that stabilizes and keeps the current flowing constant to a satisfactory level was incorporated. End effects evident on the previous trials were abolished to a satisfactory level and the degree of corrosion can be computed using Faraday's law also. Hence, this set-up of ACT was selected for the experiment program of the research.

Due to constraints in the laboratory, only three samples can be tested at the same time. Having this in mind, a line up of three samples was made to go about the ACT. The line-up was made taking the different variables in the research into consideration. Hence, it is assumed the line-up of samples in Table 3-9 can enable to see the effects of the three variables distinctively. Even if the number of samples are fifteen, only twelve samples are tested because the fifth line-up will only be a repetition of the fourth line-up of samples.

Figure 3-13: Trial three set-up

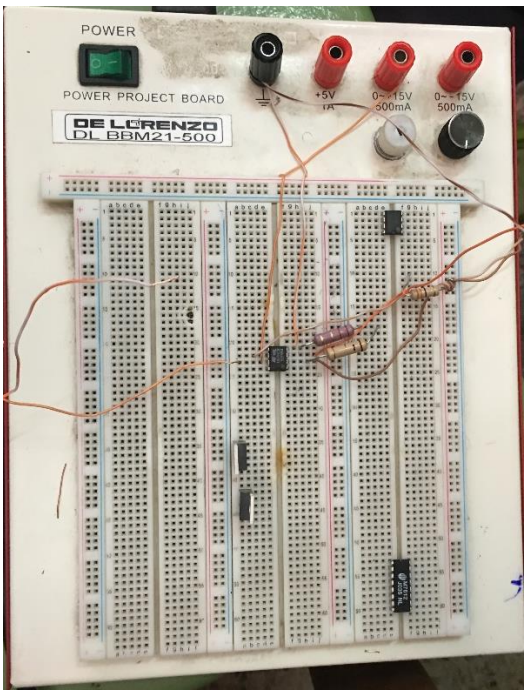

Figure 3-14: Constant current supplying circuit

Table 3-9: Line-up of samples for the ACT

Experiment Number	Type of sample-1	Type of sample-2	Type of sample-3
1st	A-28*	AP-28	C-28
2nd	B-28	BP-28	CP-28
3rd	A-28	B-28	C-28
4th	A-45	B-45	C-45

** The letter is the designation of the series and the number is the clear cover of the sample in mm.*

3.4.2 Strain measurement

The tensile stress the concrete experiences due to the corrosion of the rebar can be manifested by the strain on the surface of the concrete. Conversely, if the strain resulted by the expansion of the reinforcement is measured to good accuracy, the stress in the concrete can be captured.

The expansion (strain) of the concrete could be measured using concrete strain gauges. But this method faces a major drawback. A concrete strain gauge will measure a point strain on the location of concrete it is installed at. However, the location of maximum strain and the location of the strain gauge might not overlap. By this, the strain gauge measurement might underestimate the actual expansion taking place; hence the stress will be underestimated.

As a remedy, a loop of non-corroding metal is used to measure the expansion of the concrete. These hoop metals will circle the sample at predefined locations and strain gauges will be installed on them as shown on Figure 3-15. The contact gaps between the concrete and metal are then filled with epoxy not to lose the measurement of some strain. So, by directly measuring the strain of the hoop metal, the expansion of the concrete can be obtained.

To capture the variability of expansion of concrete, three hoop metals are provided for each sample at different locations. Two are provided 20mm below and above the boundary between the non-corroding regions and the corrosion region. The third one is installed at the center of the corroding region.

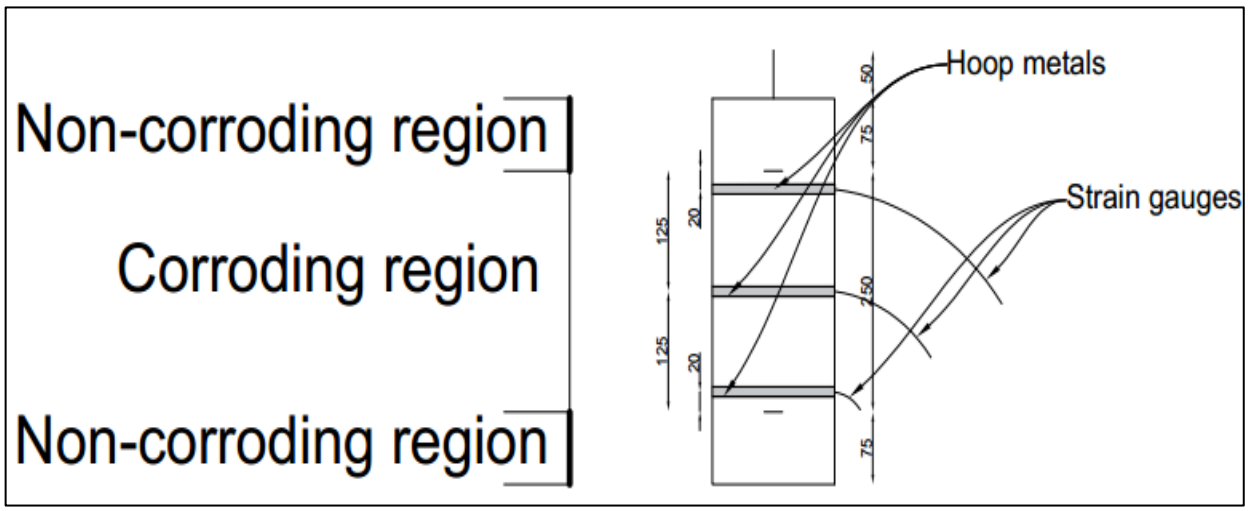

Figure 3-15: Sample preparation for strain measurement

Finally, the overall set-up of the experiment of the research became as depicted in Figure 3-16.

To avoid the effect of one sample's corrosion product on the other, all three samples in the test will be soaked in three different plastic containers.

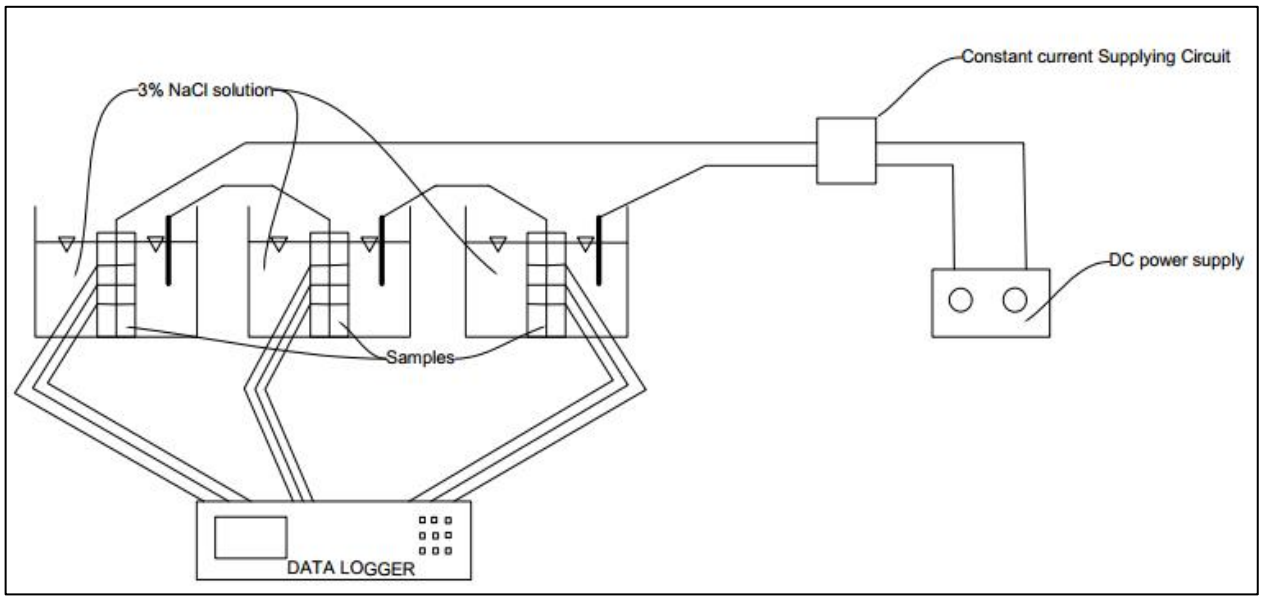

Figure 3-16: Schematic ACT set-up

Figure 3-17: Samples preparation before ACT

To prevent the saline solution from reaching the strain gauges, plumber's putty (hydrophobic material) was applied to the location of the strain gauges as depicted in Figure 3-17. Then finally a silicon gasket was smeared around the concrete and plumber's putty interface to ensure further protection from water ingression.

Accordingly, all ACTs were carried out with the set-up given in Figure 3-16. Figure 3-19 shows the first line of experiment. In all plastic containers, graphite cathodes (Figure 3-18) with equal dimensions are installed.

Figure 3-18: Graphite rod cathode

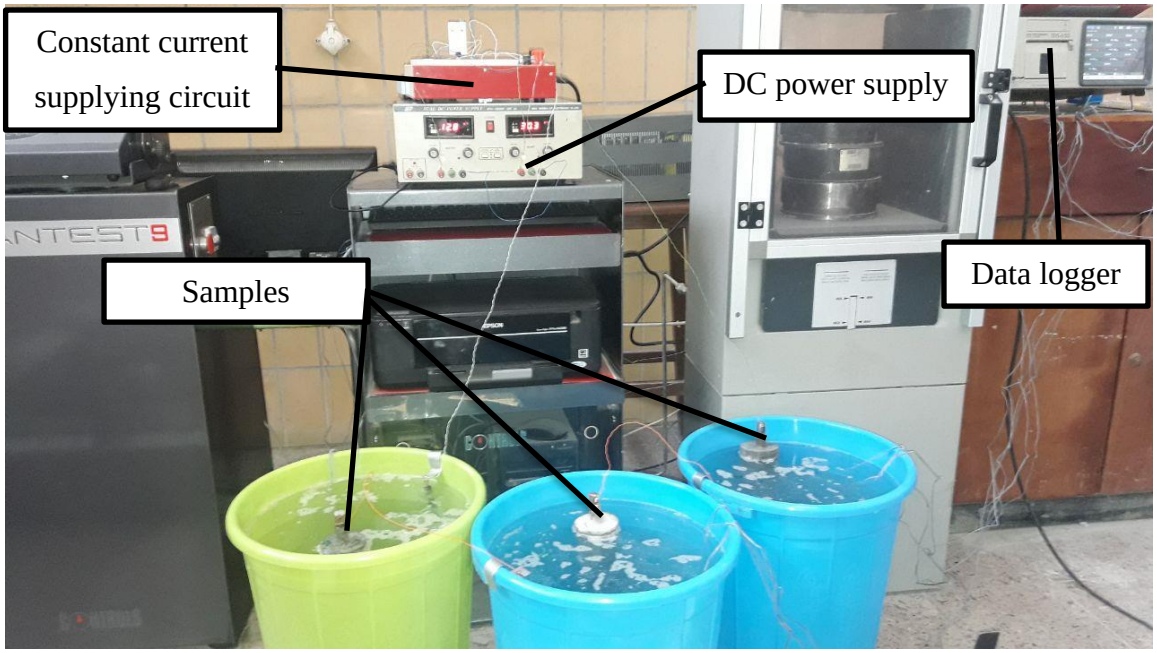

Figure 3-19: Experiment set-up

3.4.3 Cleaning of the rebars

After the ACT, the rebars from each sample are taken out and cleaned according to ASTM G 01-03. The standard recommends three types of cleaning; mechanical, chemical and electrolytic. To this research, chemical cleaning was selected because it is relatively simple and does not require providing high current density as in the electrolytic methods.

There are six possible solutions put forward in ASTM G 01-03 to wash and clean iron from corrosion products, from these a solution composing of 200gm NaOH, 20gm zinc powder and reagent water (deionized water) as depicted in Figure 3-20 was selected because the chemicals are available at large. In selecting this solution, it is required to soak the rebars in the solution for 30-40 minutes at a temperature ranging from 80-90^{o}C as shown in Figure 3-21. This temperature was achieved by a water bath. After that, the rebars were washed with tap water and allowed to dry in an open oven at 130^{o}C as illustrated in Figure 3-22 until the surface moisture on the rebars is no more: this was to minimize any further corrosion due to their exposure to moisture. Once the rebars dried, their mass was measured with a balance of 0.1gm accuracy. Then the mass losses of each rebar can be calculated as the mass of each rebar was measured before casting the concrete samples using the same balance.

Figure 3-20: Preparation of the solution for cleaning the corrosion products

Figure 3-21: Rebars soaked in the solution

Figure 3-22: Rebars drying in the oven

CHAPTER 4 RESULT AND DISCUSSION

4.1 General Information

This chapter is concerned with presenting the experimental findings and their respective discussions. In the ACT carried out, it was found that there was some variation in current delivered to the samples (maximum of 20mA). Due to this and the fact that Faraday's law assumes 100% efficiency of the current supplied, predicting the degree of corrosion using Faraday's law will not give accurate figures. However, the figures from Faraday's law are given to compare them to the actual mass loss. The gravimetric measurements were taken after a thorough chemical cleaning of the rebar samples; hence, the degree of corrosion was computed from these measurements. The ACTs were carried out in four line-ups due to the unavailability of strain gauges and channels for measurement on the data logger. It was later found that Channel 03 and 08 on the data logger did not work for strain measurement. Therefore, the remaining eight channels were used to measure the expansion experienced by the concrete during corrosion. As a result of this, strain measurement at all three locations was not taken.

The four ACTs were carried out according to the set-up devised. At the inception of each experiment, the concrete samples connected in series were supplied with 120mA of direct current. This is about a current density of $94\mu A/cm^2$ being delivered to the samples. But during the experiment, some variation in current was witnessed and it was adjusted. The maximum variation found to occur was 20mA. This implies that the current density may have varied between $78\mu A/cm^2$ to $110\mu A/cm^2$ in these instances while remaining $94\mu A/cm^2$ for the most part of the experiments.

4.2 Mass loss of rebars

The rebars in the concrete samples were cleaned and dried as discussed in the previous chapter before their masses were measured. Afterward the mass loss of each rebar was calculated. The rebars were initially numbered and their masses measured before the samples were cast. The rebar designation in each line up of experiments are given in Table 4-1.

Table 4-1: Rebars in each experiment

Series	Experiment-1	Experiment-2	Experiment-3	Experiment-4
A	1 & P1	-	3	2
B	-	7 & P2	8	6
C	9	P3	11	12
Duration (days)	*3.86*	*6.66*	*5.68*	*18.66*

The time span each experiment took is different. This is mainly due to the variability of samples in each line of experiment the time span of each experiment is depicted in Table 4-1.

Table 4-2: Mass loss of rebars

Bar No	Initial mass (gm)	Final mass (gm)	Δm (gm)	Δm (%)
1	689.1	684.2	4.9	0.711%
2	689.1	672.4	16.7	2.423%
3	696.5	689	7.5	1.077%
6	691.2	682.7	8.5	1.230%
7	686.4	678.9	7.5	1.093%
8	695.2	680.1	15.1	2.172%
9	696.1	694.4	1.7	0.244%
11	691.6	688.9	2.7	0.390%
12	684.5	680.6	3.9	0.570%
P1	745.3	740.8	4.5	0.604%
P2	735.4	723.2	12.2	1.659%
P3	737	730.9	6.1	0.828%

The percentage of mass loss is given in Table 4-2 in comparison to the original mass of the rebars; it gives the percentage of mass of each reinforcement that was consumed in the ACT. Hence, it is the degree of corrosion that was reached by the concrete samples when the concrete showed surface cracks.

4.3 Results of ACTs

4.3.1 General information

The strain development due to corrosion of embedded reinforcement follows a certain trend. Figure 4.1 can clearly depict the mechanism of stress build up due to corrosion.

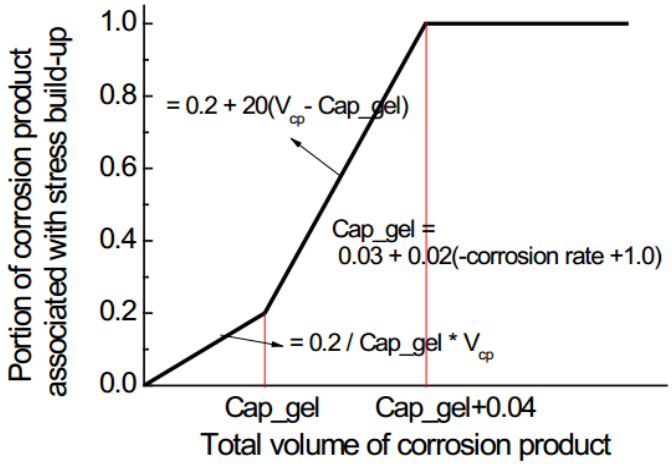

Figure 4-1: Simultaneous penetration of corrosion gel with build-up stress model. [24]

Three distinct phases can be seen from the graph given above. Initially as the corrosion of the embedded rebar begins, the liquid portion of the corrosion products will migrate into the pores and microcracks. This process creates relatively lower stress as surface tension of the fluid will not come into play and the pores are empty of corrosion products.

As time goes on, the pores will get occupied and surface tension of the liquid will be harnessed in the partially filled pores. At this stage, the stress with in increases rapidly until cracking occurs. And after cracking, the corrosion products can escape the concrete keeping the stress to an approximate constant.

4.3.2 Experiment-1

The first line of experiment was composed of A-28, AP-28 and C-28 samples. The “A” samples (A-28 and AP-28) were 42 days old while the “C” sample was 37 days old measured from the day of casting. Three hoop metals with strain gauges attached to them were installed on the three predefined locations as seen in Figure-3.17. But due to the available channels on the data logger at the time, measurement was being taken from only two of the three strain gauges for all three samples.

All three samples exhibited cracking when they were checked three days after the beginning of the ACT. (Figure 4-2 and 4-3)

Figure 4-2: Samples after the completion of ACT (AP-28, A-28 and C-28 respectively)

The dark or light green material on the surfaces of the samples is the flowing portion of the corrosion product.

Figure 4-3: Crack pattern of the samples

The strain measurements from each sample were plotted against time and are shown in Figure 4-4, 4-5 and 4-6. They were taken from the middle and bottom hoop metal for all three samples.

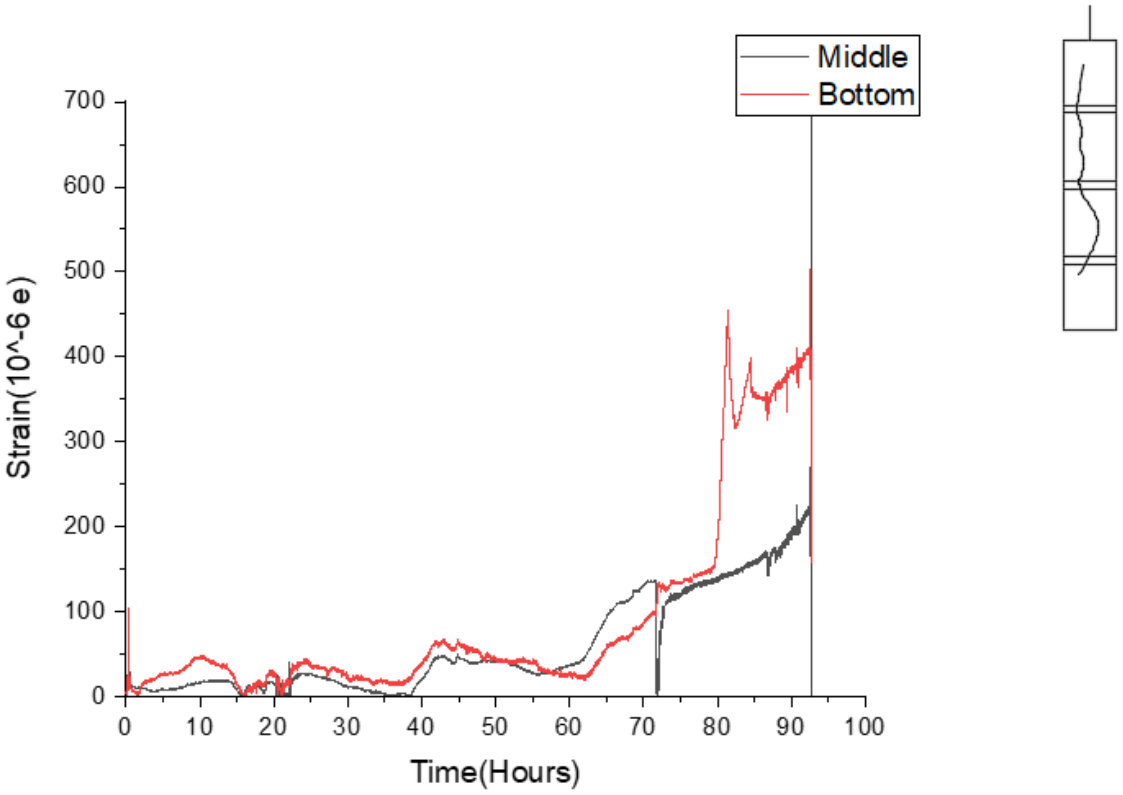

Figure 4-4: Strain measurement and crack pattern of A-28

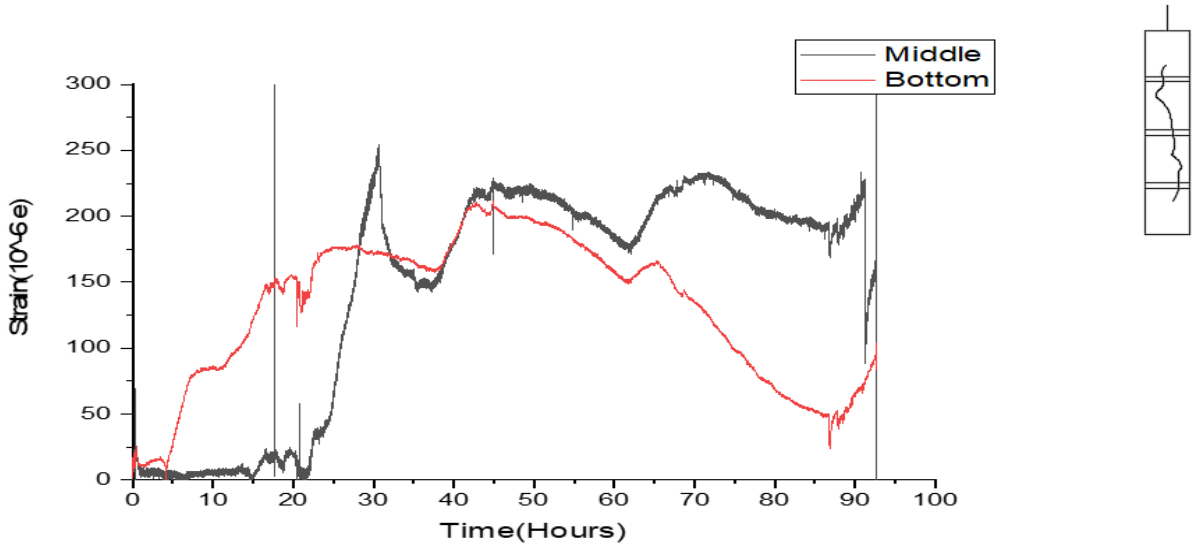

Figure 4-5: Strain measurement and crack pattern of AP-28

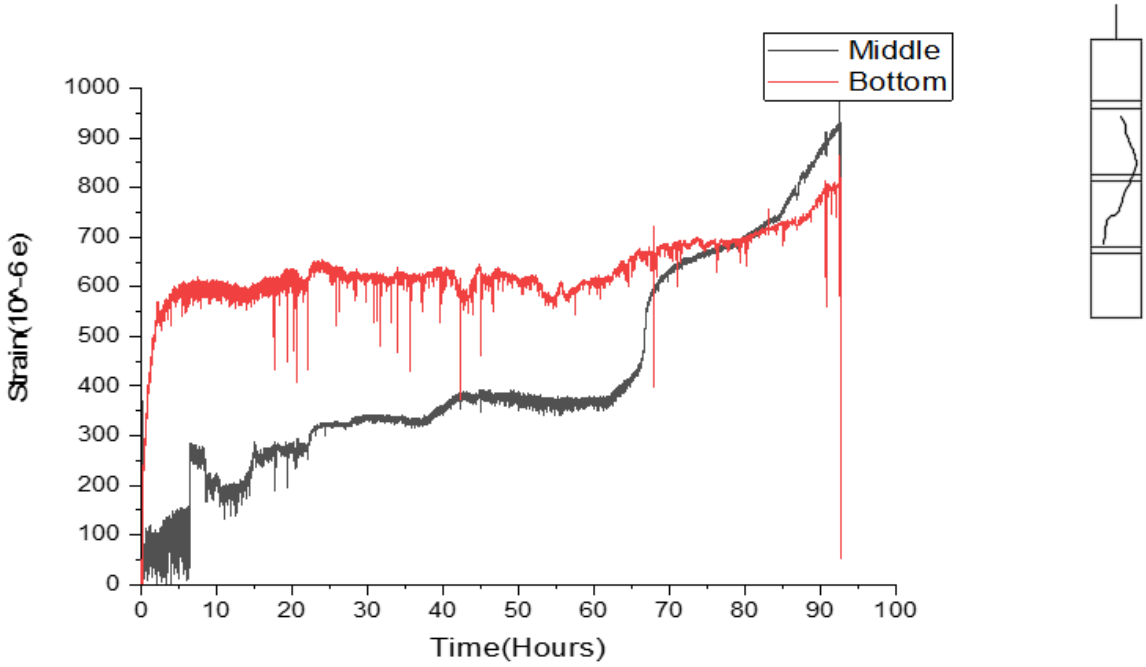

Figure 4-6: Strain measurement and crack pattern of C-28

4.3.3 Experiment-2

This experiment had similarly three samples from two different water- cement ratios. It included CP-28, BP-28 and B-28. The "C" sample was 42 days old and the two "B" samples were 43 days old measured from the day of casting. Similar to the first experiment, middle and bottom strain readings only were taken.

Figure 4-7: Samples after the completion of ACT (B-28, BP-28 and CP-28 respectively)

The samples' surfaces were then washed using tap water to see the crack patterns.

Figure 4-8: Crack pattern of the samples

The samples were being checked for cracks on regular basis. During this time, corrosion product was witnessed at the base of sample “BP-28”. This implies that all the corrosion products are not utilized to cause expansion on the concrete. Samples “CP-28” and “B-28” showed crack after four days but the remaining sample was seen to crack after six days. (Figure 4-7 and 4-8)

The strain measurements from each sample were plotted against time as illustrated in Figure 4-9, 4-10 and 4-11.

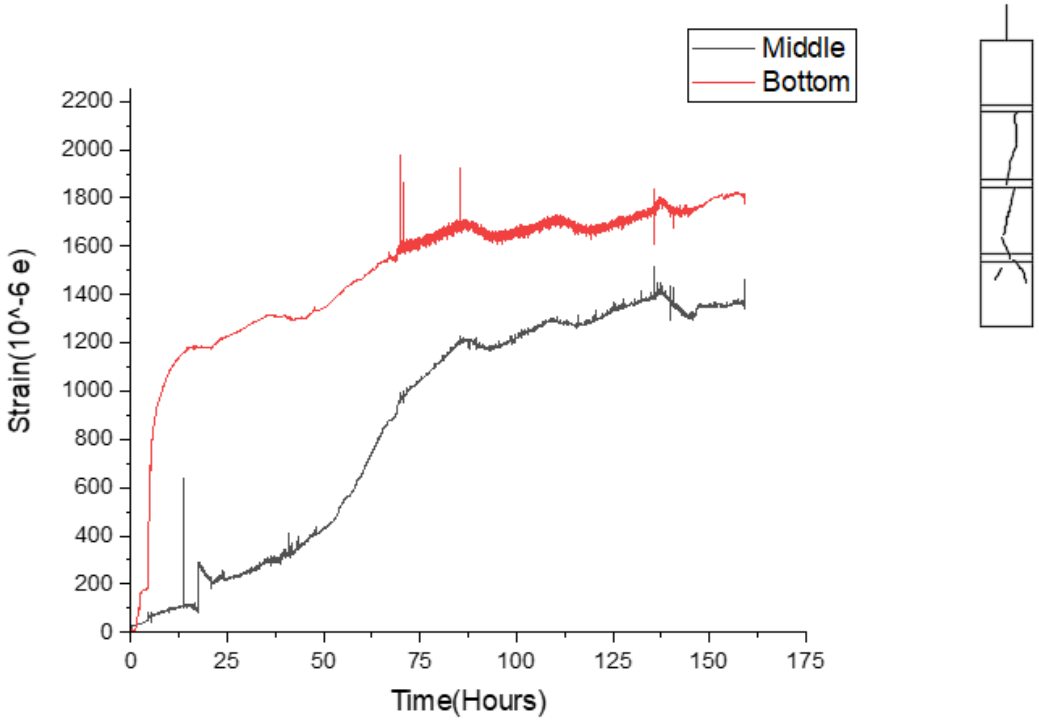

Figure 4-9: Strain measurement and crack pattern of B-28

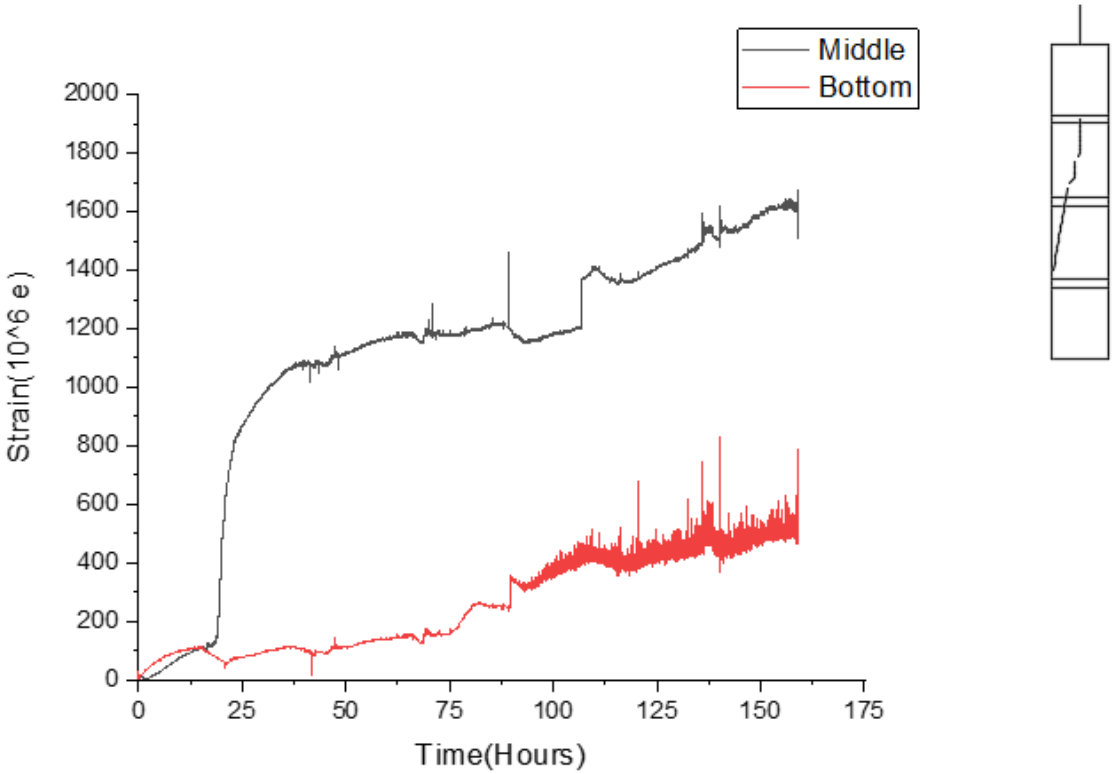

Figure 4-10: Strain measurement and crack pattern of BP-28

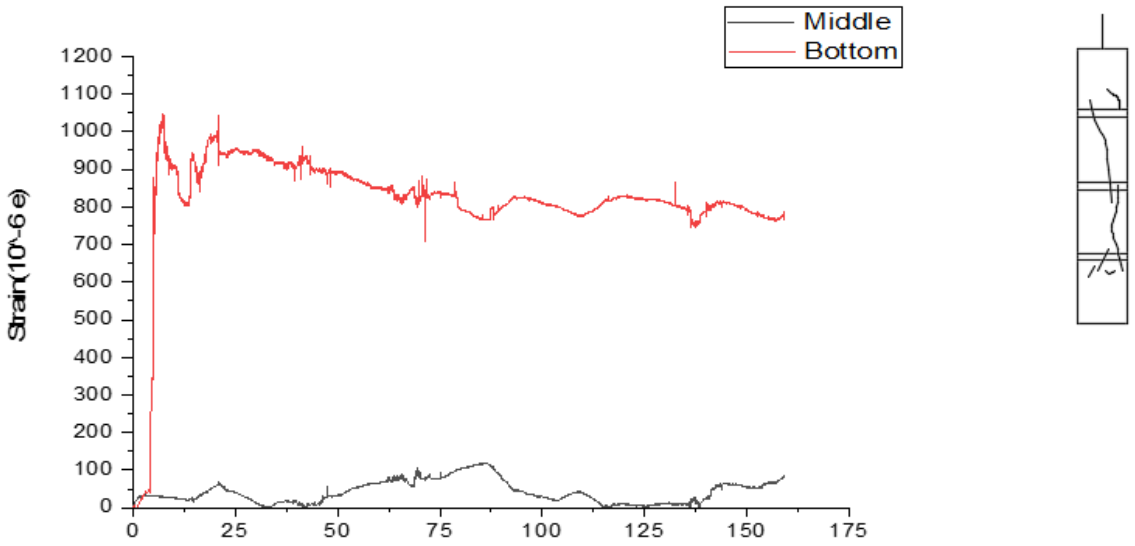

Figure 4-11: Strain measurement and crack pattern of CP-28

4.3.4 Experiment-3

This was the ACT of "A-28", "B-28" and "C-28" samples. At the inception of the experiment, sample "A-28" was 54 days old, sample "B-28" was 50 days old and sample "C-28" was 49 days old measured from their respective days of casting. All samples did not show any kind of cracking on the first two days. Then all samples were found to show cracks after four days as shown in Figure 4-12. During the observation of the samples, it was evident that sample "C-28" had some degree of end effect on the upper surface of the sample. Hence, some portion of the lost mass of the rebar was not involved in inducing hoop strain on the concrete.

Hoop metals were installed at the three location on each sample. But unlike the two previous experiments, eight measuring channels were available, hence; all three strain gauges from samples "A-28" and sample "B-28" were used to measure strains at their respective locations. But for sample "C-28" only the top and middle strain measurements were taken. Around 14 hours from the beginning of the ACT, power in the laboratory was off and unfortunately the back-up generator was not also up and running. At this time, all measurements from all three samples show a drop in strain to almost zero value due to the interruption of the current flow.

Figure 4-12: Crack pattern of the samples

The strain measurements of the samples are drawn against time as depicted in Figure 4-13, 4-14 and 4-15.

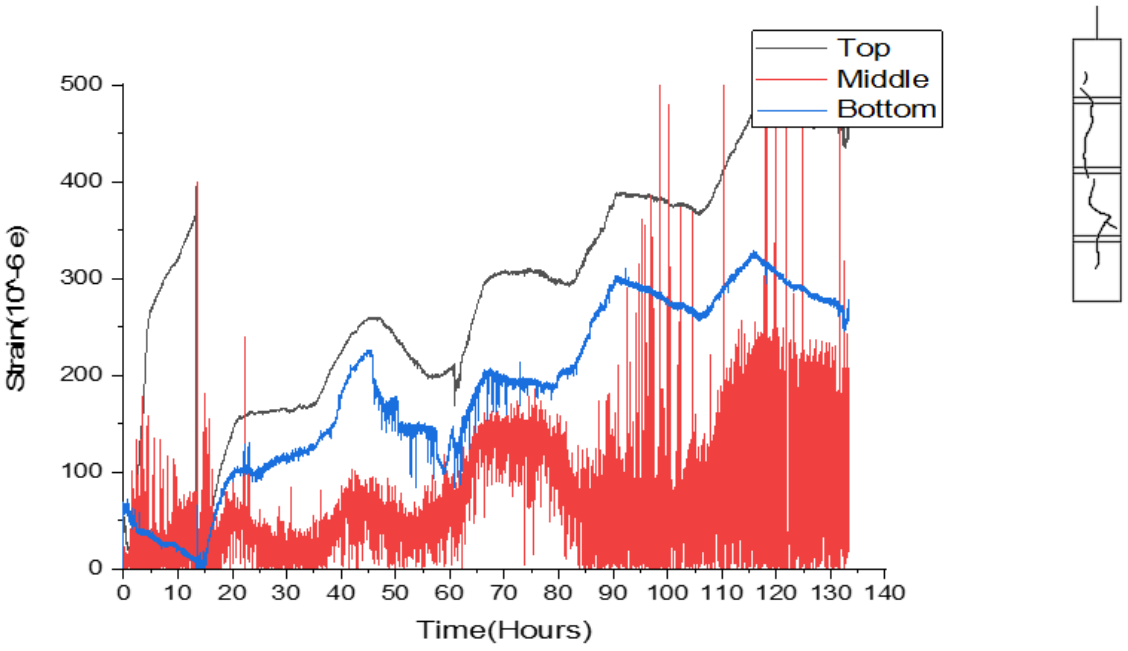

Figure 4-13: Strain measurement and crack pattern of A-28

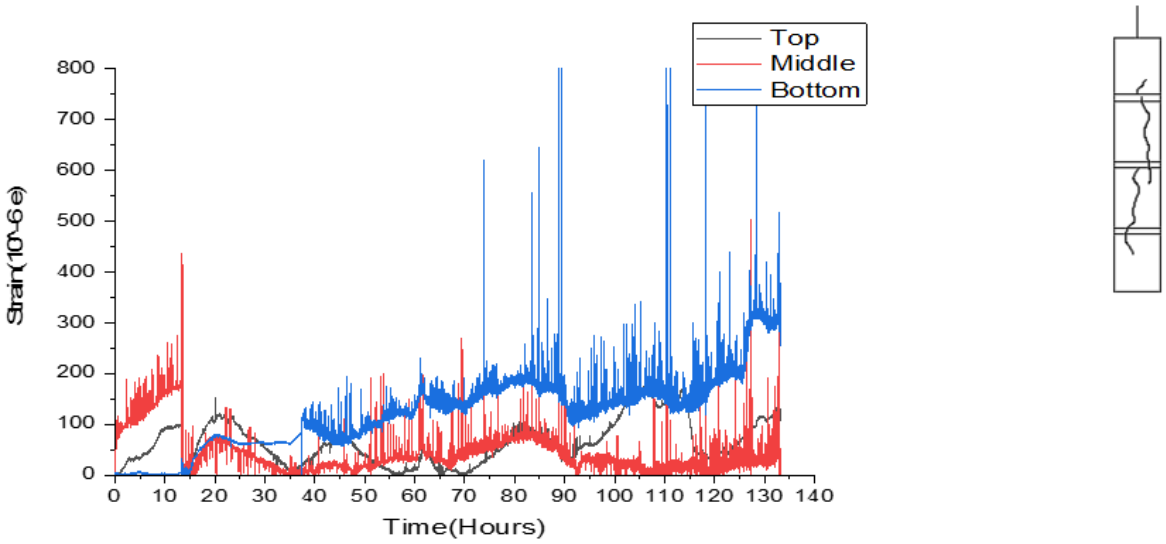

Figure 4-14: Strain measurement and crack pattern of B-28

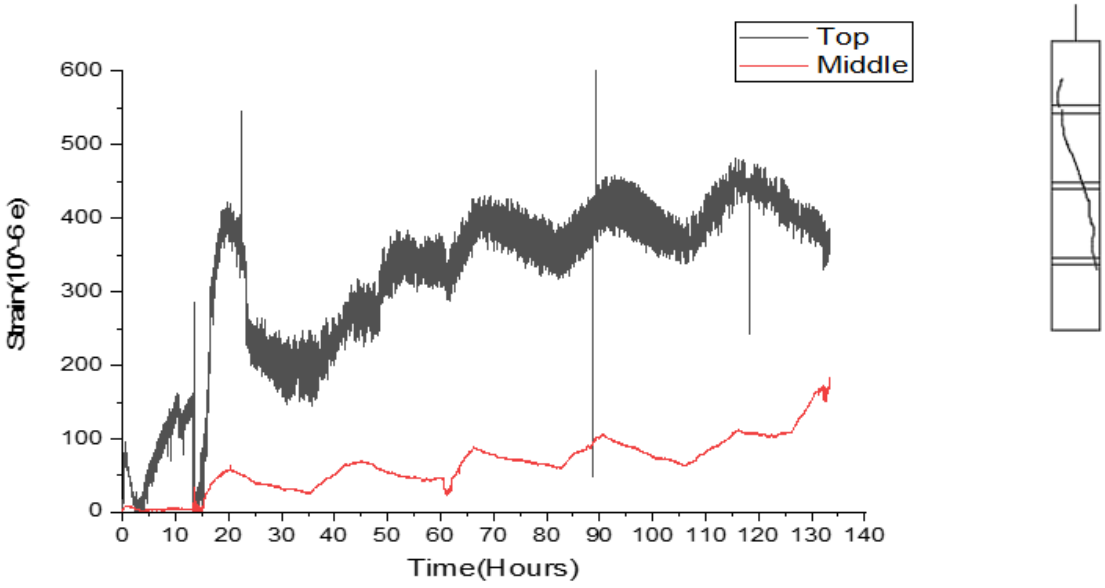

Figure 4-15: Strain measurement and crack pattern of C-28

4.3.5 Experiment-4

This was the final ACT performed and it involved "A-45", "B-45" and "C-45" samples. Sample "A-45" was 62 days old, sample "B-45" was 58 days old while sample "C-45" was 57 days old. Hoop metals were installed at the predefined locations for all samples but strain reading was taken from the middle and bottom strain gauges for sample "B-45" while for the remaining two measurements from all three strain gauges were taken.

The samples were observed but they did not show any visible crack for 17 days. However, 2 days later it was found that all samples have cracked as depicted in Figure 4-16.

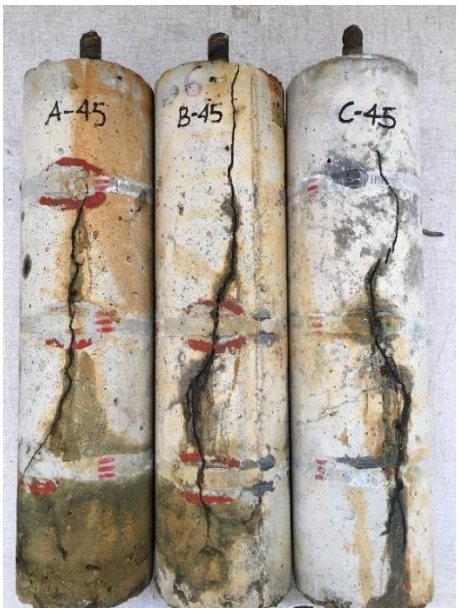

Figure 4-16: Crack pattern of the samples

The strain measurements from the samples are plotted against time as shown in Figure 4-17, 4-18 and 4-19

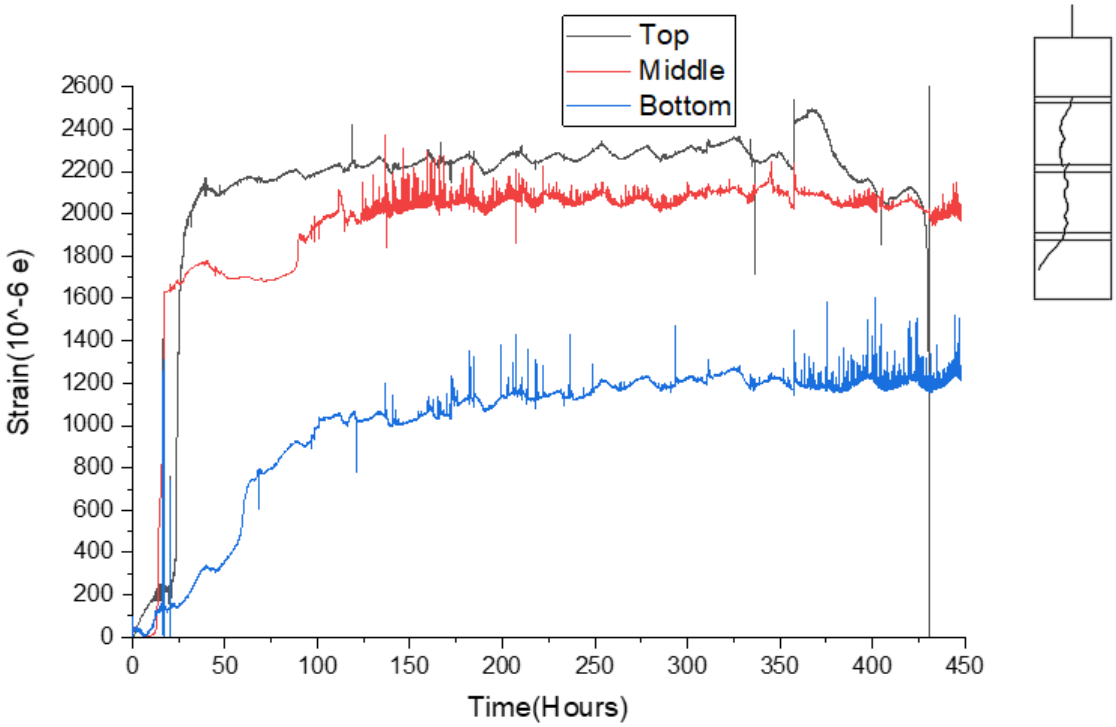

Figure 4-17: Strain measurement and crack pattern of A-45

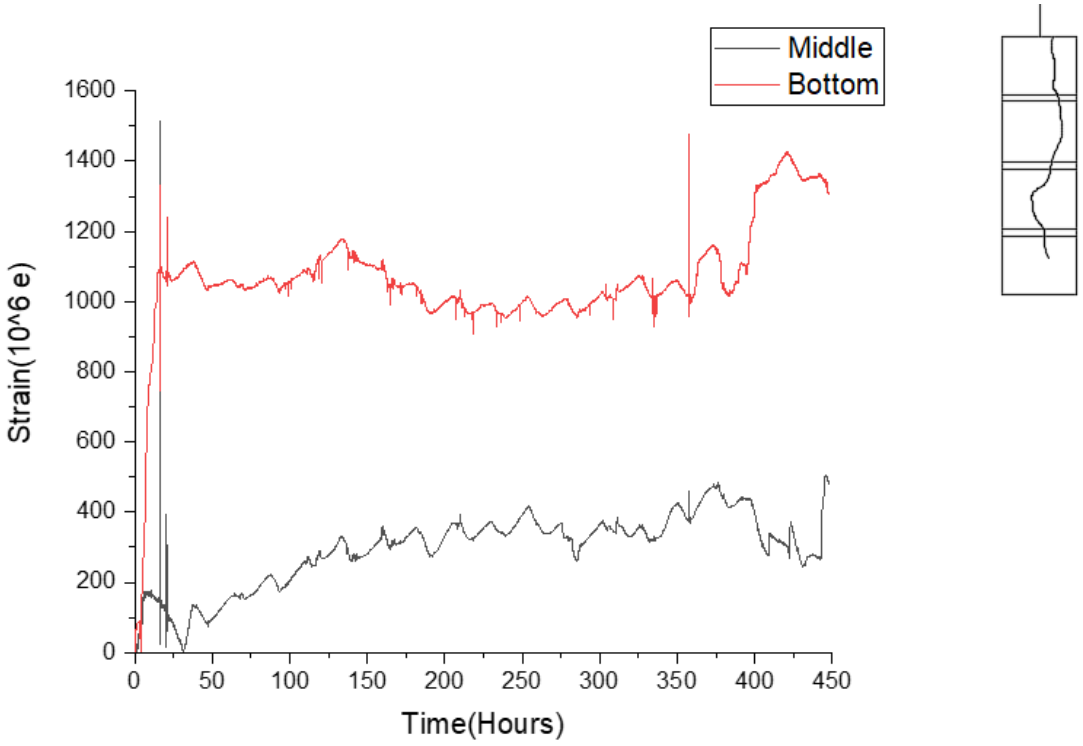

Figure 4-18: Strain measurement and crack pattern of B-45

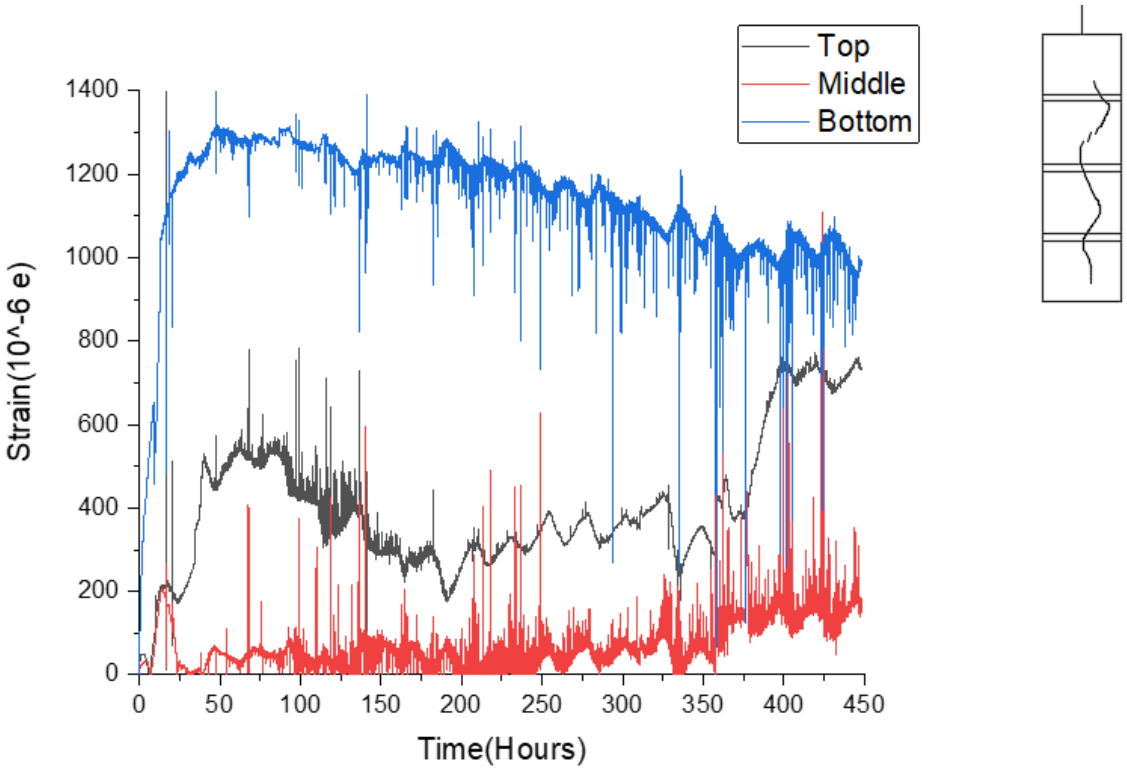

Figure 4-19: Strain measurement and crack pattern of C-45

4.4 Effect of water to cement ratio

To see the effect of water to cement ratio on the strain induced due to corrosion of the reinforcement, the average strains from the samples are plotted together. The effect is seen for the two cover thicknesses studied in the research.

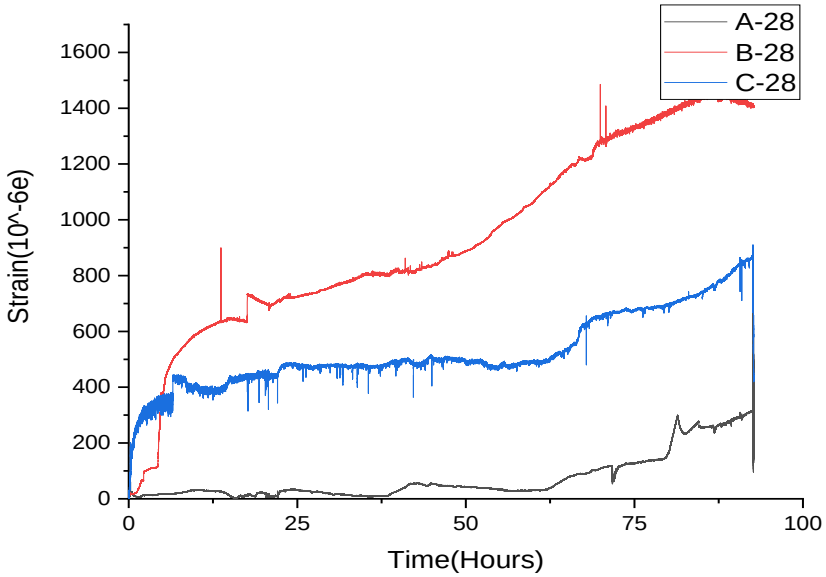

Figure 4-20: Average strain development of A-28, B-28 and C-28

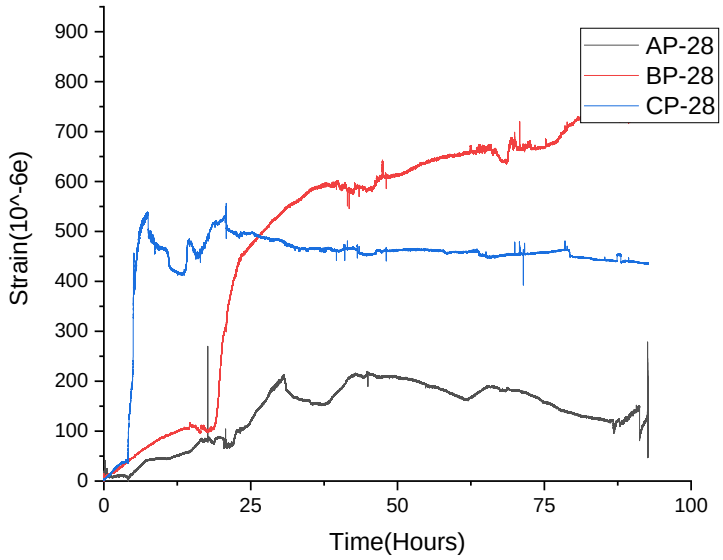

Figure 4-21: Average strain development of AP-28, BP-28 and CP-28

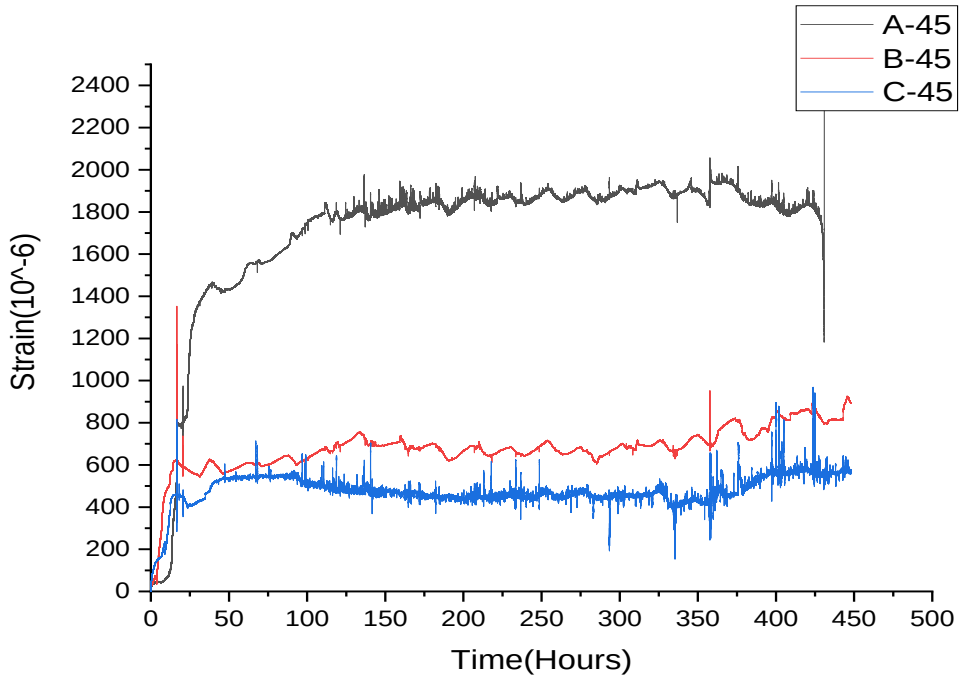

Figure 4-22: Average strain development of A-45, B-45 and C-45

For samples with 28mm clear cover (for both deformed and plane bar samples), Figure 4-20, 4-21 and 4-22, there is a distinct variation that can be seen around the inception of the experiments. The strain development is very rapid for the samples with a lower water cement ratio while it is relatively gradual for samples with a higher water to cement ratio. This is mainly due to the microstructure around the corroding rebar. As the water to cement ratio lowers the porosity of the concrete lowers as well [25] ; hence, the liquid portion of the corrosion products will not have room to fill. As a result, this creates a sudden strain rise on the sample after the ACT starts. This effect is seen well on C-28 and CP-28 samples.

However, for samples with 45mm clear cover the strain development is quite different from the ones with the lower clear cover. A-45 showed a great building up of strain earlier than any of its counterparts. This effect was also witnessed in experiments of Oh et al, 2009. This is due to the availability of oxygen at the corroding bar. For the sample with the highest water to cement ratio, the porosity is high in turn ensuring enough supply of oxygen to start and continue the corrosion of the rebar. Conversely, the expansion experienced by the sample is greater. But for lower water to cement ratio samples the oxygen supply to the anode (reinforcement) is limited. Due to this, the corrosion induced

strain of the samples takes time to develop and the magnitude of the strains were seen to be much lower for B-45 and C-45.

4.5 Effect of the surface nature of the reinforcement

There were two types of reinforcement used in the research (deformed and equivalent plane bar) and the strain measurements from the samples containing these two types of rebars showed variation.

For all three water to cement ratios the samples with plane bars showed a relative delay in the development of strain. This is possibly due to the delay of initiation of corrosion on smooth surfaces compared to rough ones as smooth surfaces are more thermodynamically stable. [6] The delays can be seen in Figure 4-23, 4-24 and 4-25.

Nevertheless, the strains in samples with plane bars increase somewhat drastically after some time passes and even surpasses the strain of deformed bar sample with water to cement ratio of 0.65. Probably, it is due to the difference in porosity around the corroding rebars. For the plane bars, the concrete-rebar interface is smooth and has relatively lower porosity compared to the deformed counterparts. As a result, the samples with deformed bars have a larger corrosion accommodating region than the samples with plane bars.

From the graphs, it is also evident that the effect of the surface nature of the reinforcements dies out as the water to cement ratio lowers and the strain development almost becomes similar for samples CP-28 and C-28. This again can be explained by the porosity of the concrete-rebar interface.

In the contrary, for samples with higher water to cement ratio becomes significant because the porosity at the interface of concrete and deformed rebar is comparably higher to the samples containing plane bars.

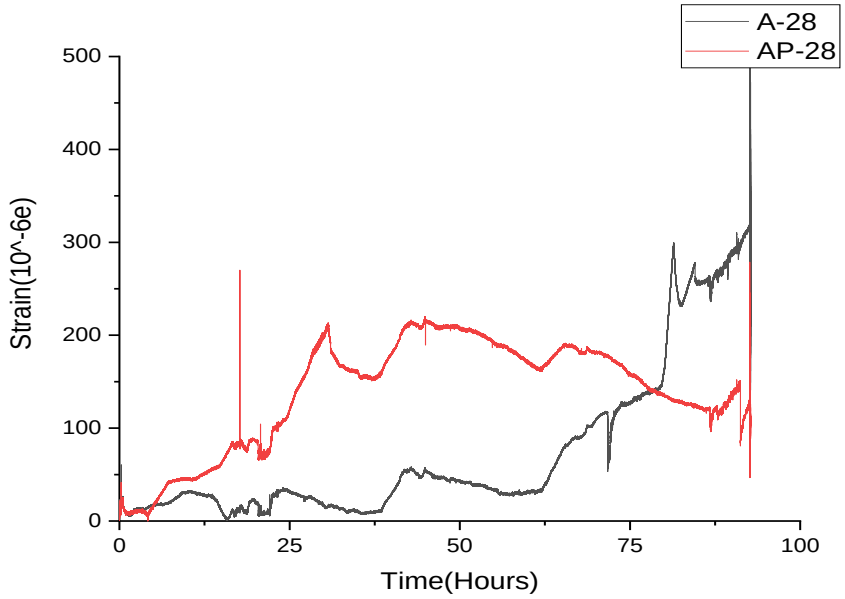

Figure 4-23: Average strain development of A-28 and AP-28

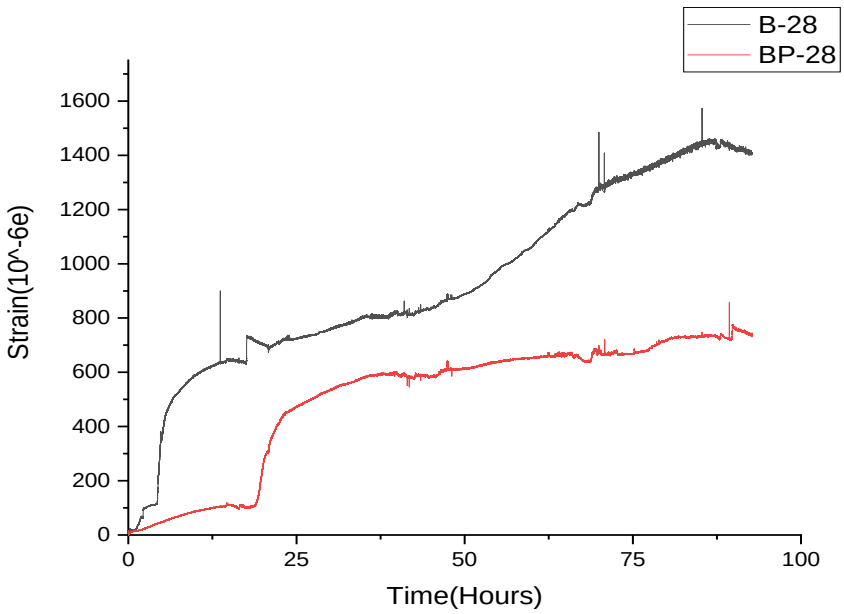

Figure 4-24: Average strain development of B-28 and BP-28

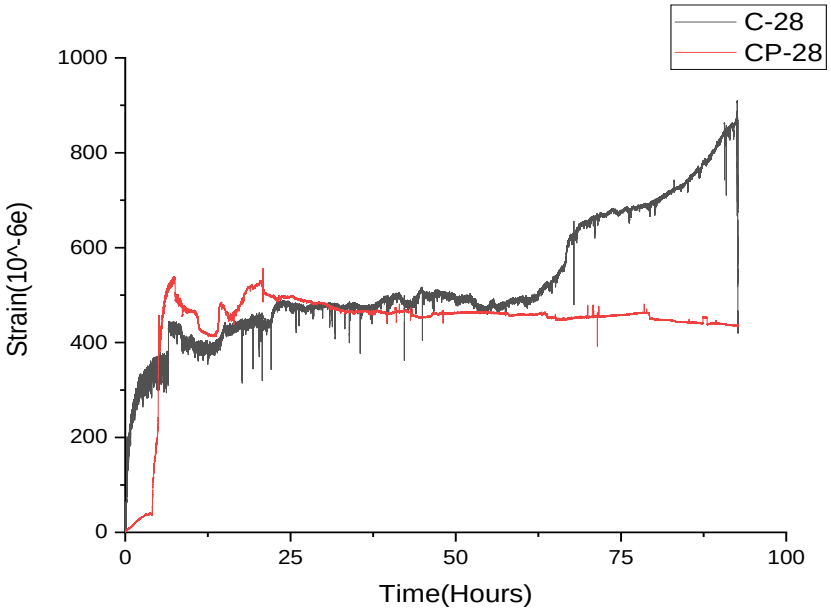

Figure 4-25: Average strain development of C-28 and CP-28

4.6 Effect of clear concrete cover

Generally, the time of crack due to corrosion extends when the clear concrete cover of the concrete specimen increases. [15] As a result, the time span for the ACT carried out for the samples with clear cover of 28mm and 45mm is very different and this makes it tough to compare the two. As a remedy, the comparison will be based on the time span it took the samples (28mm) with the lesser clear cover to crack. Accordingly, the graphs in Figure 4-26 to 4-28 are plotted.

Sample A-45 showed massively larger strain development through the time span compared to A-28. This is possibly due to the area of concrete that is withstanding the stress development as the corrosion products expand. However, the larger cover retards the ingression of oxygen and moisture, that is why the strain development for A-45 sample became slower at the beginning.

For samples B-45 and B-28, the expansion of the concrete showed similar trend at the beginning but B-28 depicted a rise while B-45 almost plateaued. This was also witnessed for samples C-45 and C-28. In fact, the average strain in C-45 and C-28 showed very similar trend for most part of the duration and C-28 sample exhibited a sudden increase in strain which is most probably when the sample is about to crack.

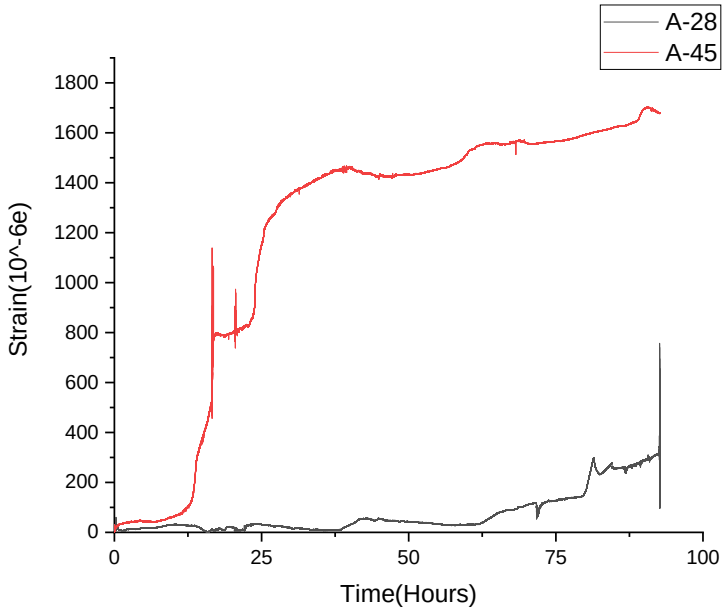

Figure 4-26: Average strain development of A-28 and A-45

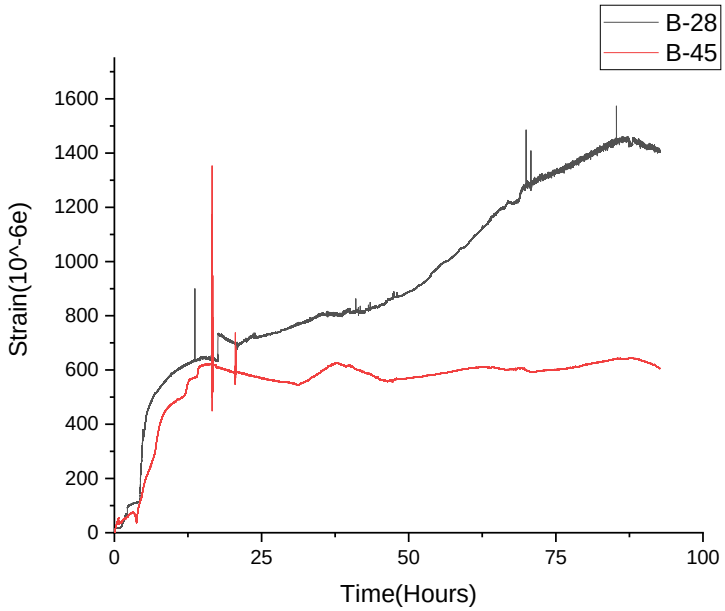

Figure 4-27: Average strain development of B-28 and B-45

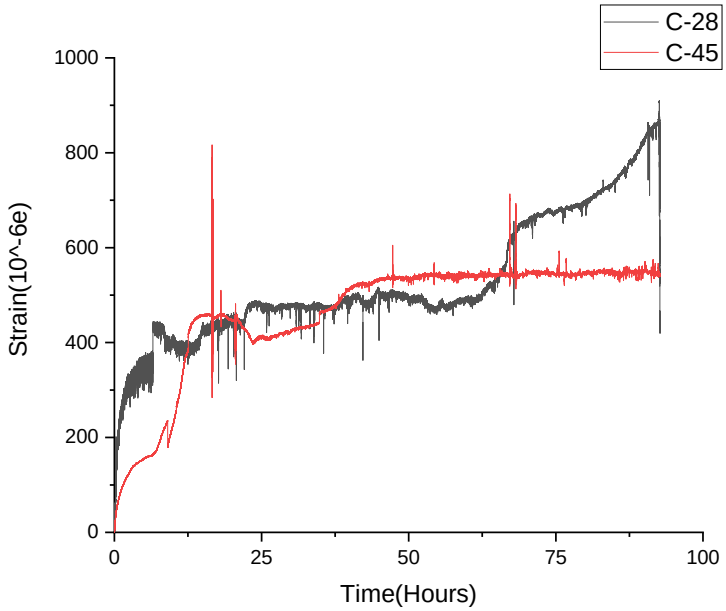

Figure 4-28: Average strain development of C-28 and C-45

CHAPTER 5 CONCLUSIONS AND RECOMMENDATIONS

5.1 Conclusion

This research dealt with the experimental analysis of the degree of expansion experienced by concrete members due the corrosion of reinforcement in them. For this, cylindrical samples with two different clear cover thickness were prepared with concrete of three different water to cement ratios. In addition, samples with an equivalent plane bar were prepared and all of the samples were exposed a controlled highly corrosive environment according to the ACT set-up devised.

The following conclusions can be withdrawn from the experimental analysis done in the research.

- Water to cement ratio affects the corrosion induced strain development. For higher water to cement ratio, the higher porosity absorbs the corrosion product to lessen the strain. This phenomenon was witnessed for samples with 28mm clear cover. But for samples with 45mm clear cover the sample with higher water to cement ratio showed more expansion.

- For the samples with 28mm clear cover of different water cement ratio, the dominant factor influencing the strain development was the porosity of the concrete. But for the 45mm clear cover counterparts, the availability of oxygen and moisture was a detrimental factor.

- Plane bars are relatively stable and are not easily attacked by corrosive agents but once corrosion starts the expansion that will develop on the concrete will be sudden and higher than samples with deformed bar. This effect is due to the microstructure at the rebar-concrete interface (it is smooth and has relatively lower porosity compared to deformed rebars) and it was more pronounced in the concrete sample with 0.65 water to cement ratio.

- As the clear concrete cover of samples increase the strain development or in general corrosion of reinforcement slows down as oxygen and moisture ingression takes much time as seen in all three samples with 45mm clear cover. However, A-45

showed a huge rise in strain compared to B-45 and C-45. This massive increment is attributed to the porosity of the concrete due to the higher water to cement ratio of A-45.

5.2 Recommendation

Based on the findings of the research the following recommendations are put forward.

- Structures reinforced with plane bars (old buildings) might get heavily damaged by the effect of natural corrosion. Hence thorough monitoring and protection schemes need to be laid down to ensure the durability of these structures.

- Construction sites need to give due attention to the appropriateness of the concrete spacers provided for the concrete members.

- For future studies, the chemical composition of the corrosion products in the samples should be studied in detail along with the variables to see to a better depth how different factors affect the expansion induced by corrosion.

- For future studies, it is recommended to study the variables in this research with different current densities much lower than used in this research.

REFERENCES

[1] Kyosti Tuutti, "Corrosion of steel in concrete," Swedish Cement and Concrete Research Institute, Stockholm, 1982.

[2] B. N. Popov, *Corrosion Engineering: Principles and Solved Problems*. 2015.

[3] H. S. Wong, Y. X. Zhao, A. R. Karimi, N. R. Buenfeld, and W. L. Jin, "On the penetration of corrosion products from reinforcing steel into concrete due to chloride-induced corrosion," *Corros. Sci.*, vol. 52, no. 7, pp. 2469–2480, 2010.

[4] G. and M. Markeset, "Modelling of reinforcement corrosion in concrete-State of the art," *Smartpipe.Com*, 2008.

[5] J. Guthrie, B. Battat, and C. Grethlein, "ACCELERATED CORROSION TESTING," vol. 6, no. 3, pp. 11–15.

[6] R. T. Leon and M.-G. Jeon, "Effect of Reinforcing Bar Chemical Composition on Corrosion Resistance," 1994.

[7] C. M. Hansson, A. Poursaee, and S. J. Jaffer, "Corrosion of Reinforcing Steel Bars in Concrete," *Corros. Eng. Dig.*, vol. 18, no. 3, pp. 110–120, 2012.

[8] K. K. Sagoe-Crentsil and F. P. Glasser, "'Green rust', iron solubility and the role of chloride in the corrosion of steel at high pH," *Cem. Concr. Res.*, vol. 23, no. 4, pp. 785–791, 1993.

[9] E. Sola, J. Ožbolt, and G. Balabanić, "Modelling Corrosion of Steel Reinforcement in Concrete: Natural vs. Accelerated Corrosion," no. June, 2016.

[10] T. A. El Maaddawy and K. A. Soudki, "Effectiveness of Impressed Current Technique to Simulate Corrosion of Steel Reinforcement in Concrete," no. February, pp. 41–47, 2003.

[11] E. Gebreyouhannes and K. Maekawa, "Nonlinear gel migration in cracked concrete and broken symmetry of corrosion profiles," *J. Adv. Concr. Technol.*, vol. 14, no. 6, pp. 271–286, 2016.

[12] S. Ahmad, "Techniques for inducing accelerated corrosion of steel in concrete," *Arab. J. Sci. Eng.*, vol. 34, no. 2 C, pp. 95–104, 2009.

[13] C. Andrade, C. Alonso, and F. Molina, "Cover cracking as a function of bar corrosion: Part I-Experimental test," *Mater. Struct.*, vol. 26, pp. 453–464, 1993.

[14] T. A. El Maaddawy and K. A. Soudki, "Effectiveness of impressed current technique to simulate corrosion of steel reinforcement in concrete," *J. Mater. Civ. Eng.*, vol. 15, no. 1, pp. 41–47, 2003.

[15] B. H. Oh, K. H. Kim, and B. S. Jang, "Critical corrosion amount to cause cracking of reinforced concrete structures," *ACI Mater. J.*, vol. 106, no. 4, pp. 333–339, 2009.

[16] Z. Wang, X. Y. Jin, N. G. Jin, X. L. Gu, and C. Q. Fu, "Cover cracking model in

reinforced concrete structures subject to rebar corrosion," *J. Zhejiang Univ. Sci. A*, vol. 15, no. 7, pp. 496–507, 2014.

[17] S. Altoubat, M. Maalej, and F. U. A. Shaikh, "Laboratory Simulation of Corrosion Damage in Reinforced Concrete," *Int. J. Concr. Struct. Mater.*, vol. 10, no. 3, pp. 383–391, 2016.

[18] A. Achal and N. . Chandak, "Effect of Salt Water on Mechanical Properties of Conventional and Pervious Concrete," vol. 14, no. 3, pp. 126–129, 2017.

[19] M. Pająk, "The influence of the strain rate on the strength of concrete taking into account the experimental techniques," *Archit. Civ. Eng. Environ.*, vol. 4, no. 3, pp. 77–86, 2011.

[20] ASTM Committee, "ASTM C33-03 Standard Specification for Concrete Aggregates," *Annu. B. ASTM Stand.*, vol. 04, no. 4, pp. 4–7, 2001.

[21] L. Melis, A. Meyer, and D. Fowler, "An Evaluation of Tensile Strength Testing, Research Report 432-lF," p. 96, 1985.

[22] ASTM Committee, "ASTM C78-02 Standard Test Method for Flexural Strength of Concrete (Using Simple Beam with Third-Point Loading)," *West Conshohocken*, p. 3, 2007.

[23] ASTM Committee, "ASTM G01-03 Standard Practice for Preparing , Cleaning , and Evaluating Corrosion Test," pp. 1–9.

[24] E. Gebreyouhannes, Y. Takahashi, and K. Maekawa, "A Poro-mechanical Approach for Assessing the Structural Impacts of Corrosion in Reinforced Concrete Members," *Proc. Int. Conf. Ageing Mater. Struct.*, no. December 2015, pp. 354–361, 2014.

[25] M. Abayneh, *Consruction Materials*. 1987.

ANNEX-A: MATERIAL CHARACTERIZATION

The following tests were carried out before the mix designs of the three classes of concrete were carried out.

Tests on fine aggregate

Silt content	
A (Silt height) in cm	5
B (Clean sand height) in cm	300
Silt (%)	1.67

Sieve analysis					
Sieve Size (mm)	Weight Retained (Kg)	Percentage Retained (%)	Cumulative Coarser (%)	Cumulative Passing (%)	ASTM standard Passing
9.5	-	-	-	100.00	100
4.75	0.0000	0.0	0.0	100.0	95~100
2.36	0.0350	7.0	7.0	93.0	80~100
1.18	0.0900	18.0	25.0	75.0	55~85
0.6	0.1800	36.0	61.0	39.0	25~60
0.3	0.1550	31.0	92.0	8.0	10~30
0.15	0.0300	6.0	98.0	2.0	2~10
Pan	0.0100	2.0	100.0	-	0
Total	0.5000	100.0	283.0	-	-

Fineness modulus= 2.83

Moisture content	
Weight of original sample (gm)	500
Weight of oven dried sample (gm)	492.27

Moisture content= 1.57%

Dry unit weight= 1592.70 kg/m^3

Specific gravity	
Weight of oven dry sample in air (gm)	485
Weight of pycnometer filled with water (gm)	1315
Weight of the pycnometer with sample and water filled up to calibration mark (gm)	1620

Bulk specific gravity = 2.487

Saturated specific gravity = 2.564

Apparent specific gravity = 2.69

Absorption capacity = 3.09%

Tests on coarse aggregate

Moisture content	
Weight of original sample (gm)	2000
Weight of oven dried sample (gm)	1975

Moisture content = 1.27%

Unit weight	
Normal unit weight of Coarse Aggregate	1,626.01 Kg/m3
Saturated Surface Dry unit weight of Coarse Aggregate	1,582.17 Kg/m3
Dry unit Weight of Coarse Aggregate	1,555.17 Kg/m3

Specific gravity	
Weight of oven dry sample in air (gm)	4945
Weight of saturated surface dry sample in air (gm)	5010
Weight of saturated sample in water (gm)	3121

Bulk specific gravity = 2.62

Saturated specific gravity = 2.65

Apparent specific gravity = 2.71

Absorption capacity= 1.31%

Tests on reinforcement

Uniaxial tensile test							
	Length (cm)	Diameter (mm)	Mass (kg)	Yield load (KN)	Ultimate load (KN)	Yield σ (Mpa)	Ultimate σ(Mpa)
Plane	49.5	14	0.6007	88.6	104.5	575.55	678.84
Deformed	76	-	1.1748	120	140.3	575.55	678.84

ANNEX-B: MIX DESIGN

Binary mix design method is used for all water to cement ratios.

A-series

Water (kg/m^3)	190
w/c	0.65
air	2%
F/A*	0.45

**Volume of fine aggregate divided by volume of total aggregate.*

S.G-FA(SSD)	2.564
S.G-CA(SSD)	2.65

S.G-FA(SSD): Saturated-Surface Dry Specific gravity of fine aggregate

S.G-CA(SSD): Saturated-Surface Dry Specific gravity of coarse aggregate

$V_w+V_a+V_{ce}+V_f+V_c=1000$……...(B-1)

V_w : Volume of water (liters)

V_a : Volume of entrapped air (liters)

V_{ce} : Volume of cement (liters)

V_f : Volume of fine aggregate (liters)

V_c : Volume of coarse aggregate (liters)

$\frac{Vf}{Vf+Vc} = 0.45$…….....(B-2)

$Vf + Vc = 1000 - Vw - Vce - Va$……..(B-3)

From equation (B1) and (B2) we obtain,

Vc= 383.50 liters
Vf= 313.70 liters

Now that the volumes of the constituents of the concrete are known, their respective masses can be computed.

Mass of ingredients required to produce 1000liters of concrete.

Water	190 Kg
Cement	292.31 Kg
Fine Aggregate	804.34 Kg
Coarse Aggregate	1016.28 Kg

Mass of ingredients required to produce 73.54 liters of concrete (the amount required to produce the test specimens and side samples).

Constituents	Full mix	Half mix
Water	13.97 Kg	6.99 Kg
Cement	21.50 Kg	10.75 Kg
Fine Aggregate	59.15 Kg	29.57 Kg
Coarse Aggregate	74.73 Kg	37.37 Kg

The concrete mixer at the laboratory was not capable to mix the whole 73.54 liters of concrete, hence the mix is divided in to two by dividing the mass of the ingredients in to two.

The coarse aggregate gradation used for the concrete was achieved through the combination of the following aggregate sizes.

ASTM Range	Sieve size	% passing	% cumulative	% retained	Mass (Kg)
100	25	100	0	0	0
90-100	19	95	5	5	1.87
20-55	12.5	37.5	62.5	57.5	21.49
0-15	9.5	7.5	92.5	30	11.21
0-5	4.75	0	100	7.5	2.8

Total mass = 37.37 Kg

B-series

Water (kg/m^3)	190
w/c	0.5
air	2%
F/A*	0.45

**Volume of fine aggregate divided by volume of total aggregate.*

S.G-FA(SSD)	2.564
S.G-CA(SSD)	2.65

S.G-FA(SSD): Saturated-Surface Dry Specific gravity of fine aggregate

S.G-CA(SSD): Saturated-Surface Dry Specific gravity of coarse aggregate

$V_w+V_a+V_{ce}+V_f+V_c=1000$……...(B-4)

V_w : Volume of water (liters)

V_a : Volume of entrapped air (liters)

V_{ce} : Volume of cement (liters)

V_f : Volume of fine aggregate (liters)

V_c : Volume of coarse aggregate (liters)

$\frac{Vf}{Vf+Vc} = 0.45$…….....(B-5)

$Vf + Vc = 1000 - Vw - Vce - Va$…….(B-6)

From equation (B3) and (B4) we obtain,

Vc= 368.19 liters
Vf= 301.18 liters

Now that the volumes of the constituents of the concrete are known, their respective masses can be computed.

Mass of ingredients required to produce 1000liters of concrete.

Water	190 Kg
Cement	380 Kg
Fine Aggregate	772.22 Kg
Coarse Aggregate	975.70 Kg

Mass of ingredients required to produce 73.54 liters of concrete (the amount required to produce the test specimens and side samples).

Constituents	Full mix	Half mix
Water	13.97 Kg	6.99 Kg
Cement	27.94 Kg	13.97 Kg
Fine Aggregate	56.79 Kg	28.39 Kg
Coarse Aggregate	71.75 Kg	35.87 Kg

The concrete mixer at the laboratory was not capable to mix the whole 73.54 liters of concrete, hence the mix is divided in to two by dividing the mass of the ingredients in to two.

The coarse aggregate gradation used for the concrete was achieved through the combination of the following aggregate sizes.

ASTM Range	Sieve size	% passing	% cumulative	% retained	Mass (Kg)
100	25	100	0	0	0
90-100	19	95	5	5	1.79
20-55	12.5	37.5	62.5	57.5	20.63
0-15	9.5	7.5	92.5	30	10.76
0-5	4.75	0	100	7.5	2.69

Total = 35.87 Kg

C-series

Water (kg/m^3)	200
w/c	0.4
Air	2%
F/A*	0.45

**Volume of fine aggregate divided by volume of total aggregate.*

S.G-FA(SSD)	2.564
S.G-CA(SSD)	2.65

S.G-FA(SSD): Saturated-Surface Dry Specific gravity of fine aggregate

S.G-CA(SSD): Saturated-Surface Dry Specific gravity of coarse aggregate

$V_w+V_a+V_{ce}+V_f+V_c=1000$……...(B-7)

V_w : Volume of water (liters)

V_a : Volume of entrapped air (liters)

V_{ce} : Volume of cement (liters)

V_f : Volume of fine aggregate (liters)

V_c : Volume of coarse aggregate (liters)

$\frac{Vf}{Vf+Vc} = 0.45$…….....(B-8)

$Vf + Vc = 1000 - Vw - Vce - Va$…….(B-9)

From equation (B5) and (B6) we obtain,

Vc= 341.73 liters
Vf= 279.54liters

Now that the volumes of the constituents of the concrete are known, their respective masses can be computed.

Mass of ingredients required to produce 1000liters of concrete.

Water	200 Kg
Cement	500 Kg
Fine Aggregate	716.73 Kg
Coarse Aggregate	905.59 Kg

Mass of ingredients required to produce 73.54 liters of concrete (the amount required to produce the test specimens and side samples).

Constituents	Full mix	Half mix
Water	14.71 Kg	7.35 Kg
Cement	36.77 Kg	18.38 Kg
Fine Aggregate	52.71 Kg	26.35 Kg
Coarse Aggregate	66.59 Kg	33.30 Kg

The concrete mixer at the laboratory was not capable to mix the whole 73.54 liters of concrete, hence the mix is divided in to two by dividing the mass of the ingredients in to two.

The coarse aggregate gradation used for the concrete was achieved through the combination of the following aggregate sizes.

ASTM Range	Sieve size	% passing	% cumulative	% retained	Mass (Kg)
100	25	100	0	0	0
90-100	19	95	5	5	1.66
20-55	12.5	37.5	62.5	57.5	19.15
0-15	9.5	7.5	92.5	30	9.99
0-5	4.75	0	100	7.5	2.5

Total = 33.30 Kg